PROGRAMME
FOR
ATMOSPHERIC WATER SUPPLY
(PAWS)

PHASE 1
1983 - 1986 FINAL REPORT

VOLUME 3
Experimental Seeding of Nelspruit Clouds

Report to the
Water Research Commission
Pretoria, South Africa

by

Simpson Weather Associates, Inc
Charlottesville Va., USA

Cansas International Corp. (Pty) Ltd
Nelspruit, South Africa

DECEMBER 1986

133/3/88

ISBN : 0 947447 06 7
Set No : 0 947447 08 3

VOLUME III

Experimental Seeding of Nelspruit Clouds

Table of Contents

EXPERIMENTAL SEEDING OF NELSPRUIT CLOUDS

1.0 INTRODUCTION

The PAWS has as its initial objective the determination of the feasibility of augmenting rainfall in the Eastern Transvaal. The experimental philosophy is to proceed in a step-wise fashion, verifying each link in the chain of processes that may lead to increases in rainfall on the ground.

Two fundamental differences might be perceived in the approach used in PAWS compared to that of other weather modification programmes:

a. While clearly recognizing the need to acquire the ability to alter the cloud microphysics in a predictable and a repeatable manner, PAWS has devoted considerable energy and resources to determining the natural conditions under which the treated and sampled clouds existed. We have recognized, as described in Volume II, Section 4, that the scales of motion and processes larger than those confined to the interior of convective clouds range from those produced by the cloud (outflows) to planetary scales which regulate the wet and dry periods. Explicit determination of the forces operating on the cloud on all scales would entail virtually every aspect of meteorology. Such a formidable task borders on the impossible, at least for any single weather modification project. We were, however, unwilling to accept that nothing could or should be done. On the contrary, we believe that the objectives of PAWS to determine the potential for augmenting water supplies through the artificial treatment of convective storms cannot be attained without simultaneously gaining a comprehensive understanding of natural processes controlling unmodified rainfall distributions. Thus, a major component of the PAWS research is directed at two aspects other than the internal cloud microphysics:

   * how do other scales of motion directly influence and interact with attempts at artificial augmentation?

   * how do we translate any demonstrable seeding effects into water supply?

b. PAWS differs from other seeding programmes in the kind of seeding targets and treatment of the targets. New growing cells generated on the flanks of medium sized multicellular storms are seeded in a sustained fashion for up to 40 minutes after the initial seeding run.

Altering of the cloud microphysical properties requires a suitable seeding agent which will produce the desired response which in turn can be measured with available equipment. The search for such a material entailed airborne seeding trials and work in cold rooms and a cloud simulation laboratory (Emmitt, 1984; Morrison et al., 1984). The results from these tests led to the choice of dry ice as the initial seeding agent.

One method of testing the level reached in comprehending the local cloud processes is to cautiously embark upon a cloud seeding programme. To this end, a seeding experiment was commenced at Nelspruit in October, 1984. A major goal of this experiment was to see if the microphysical changes that were documented so clearly and repeatably at aircraft volume sampling scales (litres) were spreading to scales large enough to be detected using meteorological radars (scales of cubic kilometres). It was reasoned that if cloud seeding programmes are going to produce annual increases in rainfall of 10 to 15 percent, then the increases from individual storms should be at least 5 to 10 times this amount, i.e. 50 to 100 percent. Such increases, if attainable, could surely be detected in a carefully designed experiment using a single cloud or storm as the experimental unit. Section 3 of this volume presents the results from the first two seasons of the exploratory randomized seeding experiment.

A search for covariates (or concomitant measurements), whose purposes are to reduce the natural experimental variability, has revealed an apparent link between the presence of supercooled water drops at seeding levels and the level of success achieved in the seeding experiment. Here the deliberate application of a physical measurement to the statistical experiment improved results, signalling a growing understanding of cloud physics and cloud processes. It has also sharpened the definition of seedable clouds, and, with the help of the data from the 16 gauge automatic rain gauge network, allows us to make a rough first estimate of what portion of the natural rainfall is "seedable".

Recognizing that the environment of seeding targets may govern the degree or even the nature of a response to treatment, efforts have been made to evaluate the radar detected "seeding signal" in terms of the synoptic, mesoscale, and convective scales.

2.0 MICROPHYSICAL SEEDING EFFECTS (Emmitt)

The choice of a seeding material (dry ice) and delivery technique using the Learjet for the PAWS was made on the basis of research conducted during the RAIN project (Rain augmentation in Nelspruit; Garstang et al, 1981). The short term (3 to 10 minute) cloud physics response to dry ice was measured and documented during the same period. Results of the RAIN seeding studies are reviewed here briefly for completeness. A more detailed presentation can be found in Section 7.0 of Volume IV.

The seeding material chosen for the PAWS is dry ice (solid CO_2) in the form of small cylindrical pellets about 1 cm in diameter with lengths varying between 0.2 and 3.0 cm. These are dispersed from one of two 45 kg capacity bins carried inside the Learjet. Seeding rate using one bin is around 0.2 kg/sec. This amounts to about 1.3 gm of dry ice per metre of travel through a target cloud.

The principal conclusions of the RAIN microphysical seeding studies were:

a. Dry ice seeding of eastern Transvaal cumulus clouds produces concentrations of ice particles exceeding any observed natural concentrations within a few minutes of seeding

b. The ice production effectiveness for dry ice is 10^{11} to 10^{12} ice crystals per gram (laboratory and airborne tests)

c. Diffusion by the turbulence naturally present in clouds is highly effective in spreading the microphysical seeding effect throughout a large volume of the supercooled cloud.

3.0. THE EXPLORATORY RANDOMIZED SEEDING EXPERIMENT (Dixon and Mather)

The PAWS rain augmentation experiment is a randomized exploratory experiment primarily designed to :

- test the logistics of seeding methods
- determine those situations in which seeding will be most effective
- learn how better to measure these effects
- identify the strongest radar (and other) response variables
- gain a clearer understanding of cloud physics and cloud processes
- estimate the potential effect of changes in rainfall due to artificial stimulation on water supplies
- gain an understanding of the interactions of other scales on natural and artificially stimulated convective rainfall.

At this stage of the research, no attempt is being made to systematically increase rainfall on the ground.

The experiment is both confirmatory and exploratory in the sense that we wish to test the hypothesis that seeded storms behave differently from unseeded storms and that some of these differences can be detected by sensitive radars; exploratory in the sense that we do not know in advance what these difference will be.

The experiment is randomized, since randomization is recognized as a reliable cure for many experimental design problems.

3.1 Experimental target selection

The target selected for the experiment is the medium sized, isolated multicellular storm. This target was chosen for several reasons:

- the storm tracking programme readily tracks this entity
- the medium sized convective complex is almost always present on a convective day thus supplying many experimental opportunities
- rainfall and radar studies indicate that the selected target produces a significant portion of the rainfall in the Nelspruit area
- the convective complex is large enough to provide a longer lasting source of supercooled water than that found in isolated cumulus congestus clouds.

3.2 Experimental procedures

The way in which the experimental units were chosen is examined in detail in this section, since a clear understanding of these procedures must be acquired before the results of this experiment can be interpreted and evaluated. The "decision tree" shown in Fig. 3.2.0 should be of assistance here.

A radiosonde is launched at 08:00 SAST.* The radar is calibrated and Volume Scan is started at 09:00. A briefing commences at 10:30 at which time a forecast is made based upon the local sounding, and upper air and surface data received from the South African Weather Bureau. The forecasts are divided into 3 categories, "Go", "Standby" and "No Go". In the event of "Go" and "Standby" forecasts, the radar is manned.

* All times, unless otherwise noted, are in South African Standard Time, Greenwich plus 2 hours.

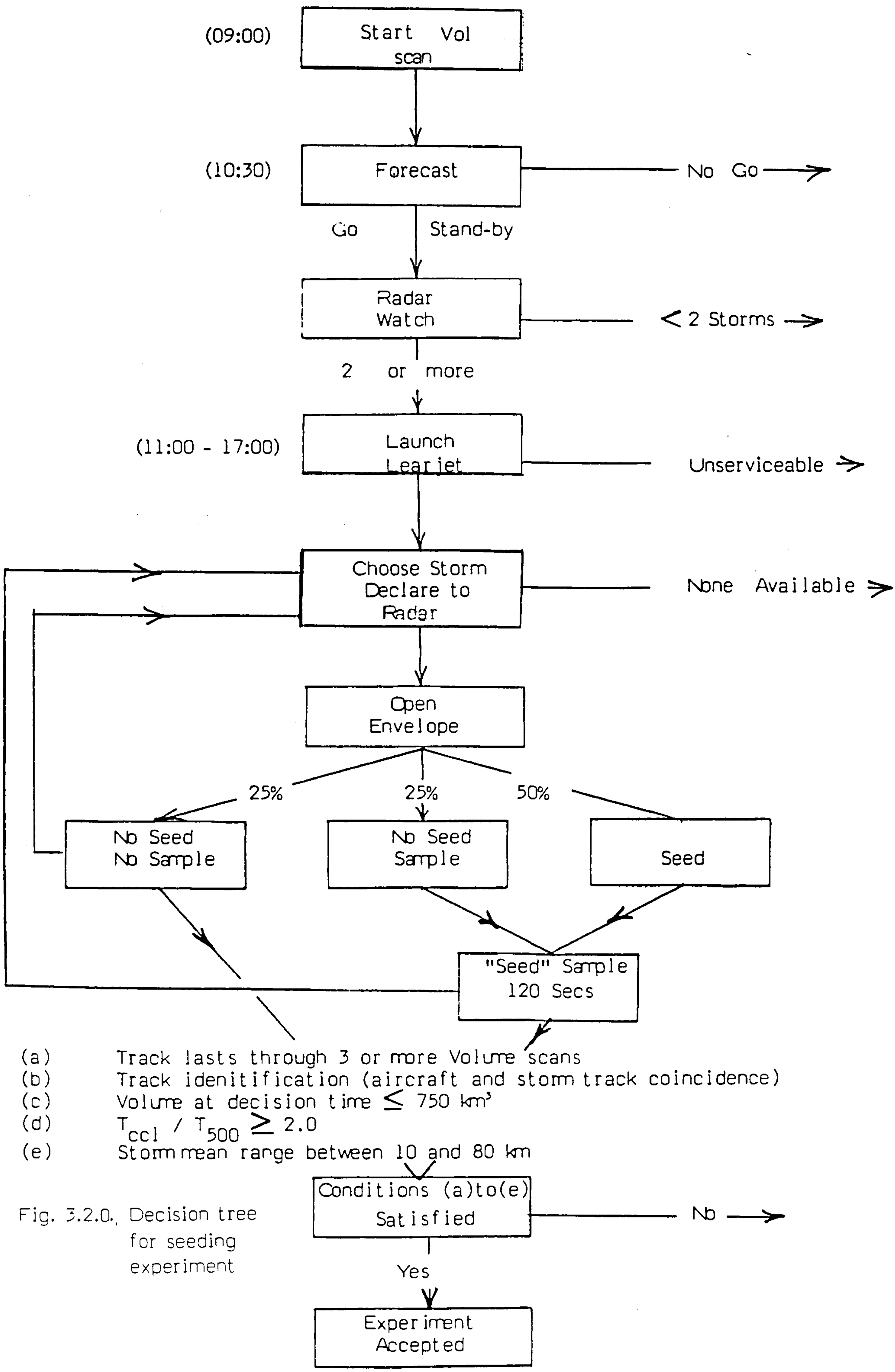

Fig. 3.2.0. Decision tree for seeding experiment

The Learjet is launched when two or more clearly separated radar echoes within the experimental area exceed reflectivity thresholds of 40 dBz. This criterion was set to avoid launches in marginal conditions, since experience has shown that when two storms are present, the probability is high that at least one experiment will be performed.

The radar operator then directs the Learjet to the strongest or most likely (isolated) target on radar. Upon reaching the storm of interest, the aircrew declares the storms an experiment if:

- one or more fresh cloud turrets are growing through the -10°C level

- the storm has a well-defined base, i.e. cloud tops not separating from their bases

- the growing turrets have reasonable dimensions, i.e. good storm width-to-height proportions and not excessively sheared.

After the aircrew have declared a target and informed the radar operator by radio, the envelopes containing the randomized instructions are opened by the radar operator or his assistant. Declaration of an acceptable target is logged as "decision time" by the aircrew and radar operator. The instructions in the envelopes lead to one of the following three courses of action:

- seed and sample (by penetrating) once each turret growing on the flank of the storm between the -5 and -15°C isotherms for a maximum seeding time of about 120 seconds (23 kg of dry ice)

- do not seed, but sample all turrets (again between the -5 and -15°C environmental temperature levels), carrying out mock seeding runs (i.e. pressing the seeding button, recording the "seeding" time but with the seeding bins de-activated) for a maximum of 120 seconds of simulated seeding.* (see footnote Pg. 6).

The randomized instructions were prepared by the WRC in Pretoria, sealed, then sent to Nelspruit. Strict accounting of the use of the envelopes was kept in Nelspruit and Pretoria. Each pair of envelopes had a number which corresponded to a case (experiment) number. Details of all operations (flight times, seeding times, storm locations) were telexed to Pretoria within 24 hours of all missions.

The data were partitioned into three groups because of concern expressed about the effects of just the Learjet on the experimental clouds (aircraft produced ice particles or APIPS, see Hobbs, 1982). Because of sample size limitations the no-seed/sample and the no-seed/no sample experiments are lumped together as no seed cases in the analyses to follow.

The selected targets were then tracked throughout their lifetimes by the project radar.

3.3 Data Analysis

The radar tapes containing the raw volume scan data and the returns from the Learjet transponder are dumped to disk. During this process "blue sky" elimination takes place, producing packed radar files. Next, 63 storm properties are computed for each volume scan sequence. The storm tracking algorithm is run on these properties, tracking the storms in time through each volume scan, and calculating a total of 244 storm track properties. A storm track commences when a volume contained by a 30 dBz contour exceeds 3 km^3 and ceases when the same volume decreases to less than 3 km^3 (see Volume IV for a detailed description of these processes).

Next the case tracks are identified by displaying the seeding aircraft track superimposed upon the storm track. Coincidence in time and space of both tracks identifies the target storm.

The seeded and unseeded storm track properties are compared by calculating:

- minima
- maxima
- arithmetic and geometric means
- standard deviations
- skewness
- inter-property correlations

The test statistic for each of the above is defined by the "seed" minus the "no-seed" differences. Only the differences in means are used in the analyses that follow.

The significances of the above differences are determined using standard re-randomization techniques. Briefly, difference distributions are generated by splitting the case pool into seed and no-seed pools, using the same randomization scheme employed in the real draw. If p % of the differences calculated from the

---

* Maximum seeding time of 120 sec refers to the actual time during which dry ice pellets are being dispersed from the dispenser at a rate of about 200 g sec^{-1}. As much as 4 kg (20 sec) of dry ice is released in each run. Turrets of a given complex may be seeded for a period of time of up to 40 min before a total of 23 kg of dry ice, or 120 sec, have been consumed (See Fig. 3.4.0).

---

re-randomization are equal to or more extreme than the values obtained in the real experiment, then p % is an appropriate measure of the unlikeliness of the actual event. For example, if the difference in mean cloud heights between the real seed and no seed cases falls within the top (or bottom) 50 differences calculated from 1000 re-randomizations, then p will be equal to or greater than 95 percent (or less than 5 percent).

3.4 Seeding Rates

Fig. 3.4.0 indicates the average seeding rates for the 1984/85 and 85/86 seasons: 60% of the maximum of 23 kg is dispersed after 15 minutes and 81% after 25 minutes (relative to decision time). This statistic should be borne in mind when viewing the seeding response data.

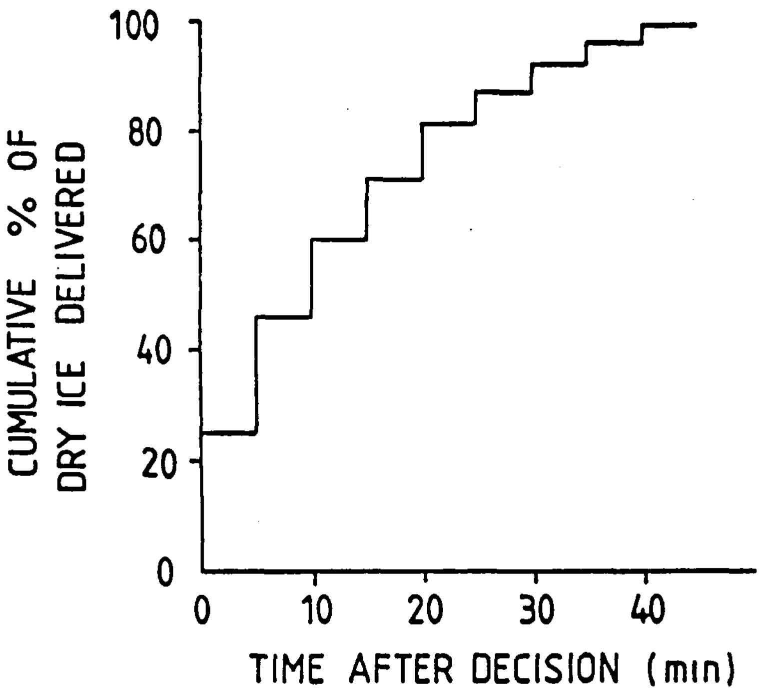

Fig. 3.4.0. Mean dry ice seeding rate - seasons 1984/85 and 1985/86. Cumulative totals represent percent of the total weight of dry ice delivered in the interval.

3.5 Seeding windows

The seeding windows that were used in this experiment are discussed below:

a. The temperature ratio partition

Fig. 3.5.0 depicts the occurrence of supercooled water drops and graupel as a function of the temperature at the convective condensation level (T_{CCL}) and the buoyancy at 500 mb (Delta T_{500}). Each circle represents a single storm in which clear images of drops were encountered. Many of these passes also contained images of graupel. Each cross represents a storm in which only images of graupel were encountered on all passes. It has been hypothesized that the release of the latent heat required by the dynamic seeding concept can only occur when supercooled water drops are present at seeding levels (Lamb et al., 1981). These data can be partitioned into cases where drops probably exist by a simple ratio of T_{CCL} to Delta T_{500} (shown in the figure). This partition includes all but one of the observed drop cases and eliminates many of the graupel only cases. Here we wish to emphasize that this partition was arrived at when considering the microphysical measurements (Section 5) and was only later applied to the radar analysis.

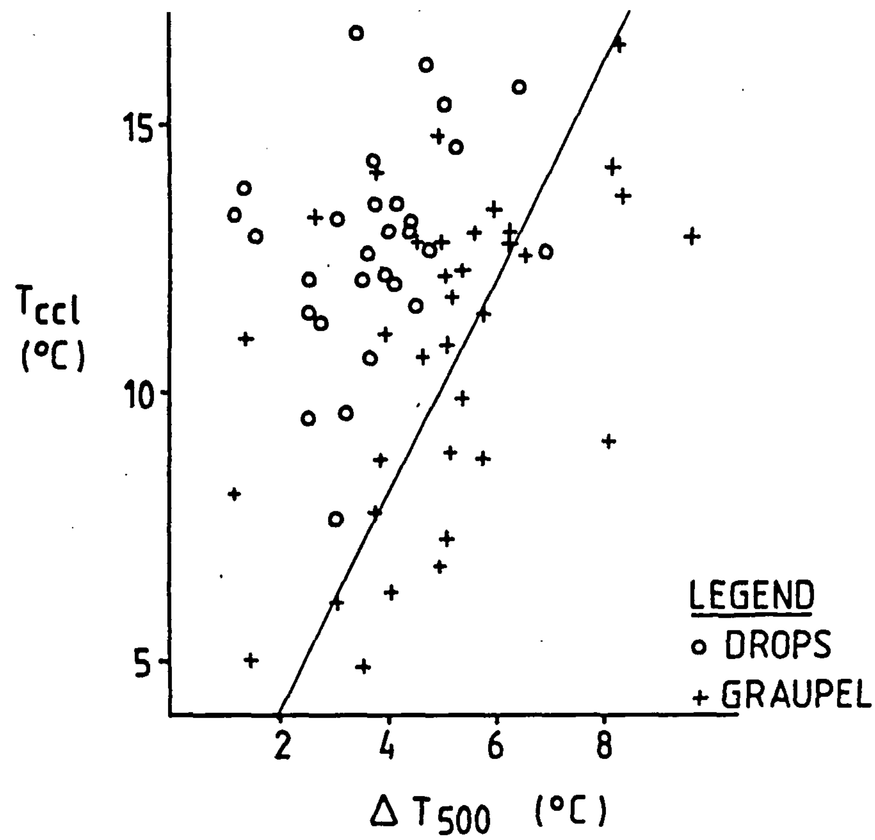

Fig. 3.5.0. First pass drop and graupel encounters plotted against convective condensation level temperatures (T_{CCL}) and 500 mb buoyancies (Delta T_{500}).

b. Storm volume at decision time

The storm tracking programme will track a squall line as a single entity, resulting in unrealistic storm areas and volumes. It was found that these extreme cases could be eliminated by restricting the storm volume at decision to 750 km^3 or less. This stratification eliminated two huge seed cases that were dominating the results to follow.

c. Radar range limitations

The study in Volume IV, Section 3.16 shows a serious degradation in the radar data beyond a range of 80 km, so only those case tracks which fell within an annulus of from 10 to 80 km radius from the radar were accepted for this analysis.

3.6 Biases

Since the seed decision is known to all project personnel, experimenter bias cannot be completely ruled out through the sampling and analysis stages that follow decision time. The objective cell tracking programme certainly helps to reduce the risk of bias slipping into the analysis procedures. All storms that are tracked through 3 volume scans or more are displayed with the aircraft track superimposed. Coincidence in time and space almost always unequivocally identified the case (experimental storm) track.

There can be no substitute for a "double blind" situation in which the aircrew, the radar operator and the analysts are unaware of the treatment until the experimental analysis is complete. We will be adopting a double blind procedure for the next experimental season.

3.7 Control parameters

Randomization does not eliminate the risk of biases resulting from unlucky or bad draws. Measures used to warn against such an outcome were:

- computing 12 control properties which should not be affected by seeding. These are:

a. mean range of storms from radar
b. storm volumes at decision time
c. peak reflectivities at decision time
d. temperatures at the CCL (T_{ccl})
e. buoyancies at 500 mb (ΔT_{500})
f. $T_{ccl}/\Delta T_{500}$ ratios

For the day of the experiment:

g. number of storm tracks
h. cumulative 3° area-time-integrals (ATI)
i. maximum storm volumes
j. maximum ratio of increase in storm volumes
k. maximum cloud tops
l. maximum reflectivities

- analysing the data from 10 minutes before decision time up to decision time

- splitting the data into two seasons. A spurious statistical response would be probable if a track property showed a high p value in one season and a low one in the next.

3.8 Results

From 106 experiments over 2 seasons, 95 storm tracks were analysed. Reasons for rejecting 11 tracks were :

- seeding at -25° C
- no aircraft tracking data
- invalid storm tracks.

After applying the following stratifications:

- mean ranges : 10 to 80 km
- storm volume at decision time: 0 to 750 km^3
- T_{CCL}/ Delta T_{500} : 2.0 or greater.

a total of 69 storm tracks remained, 32 seeded and 37 unseeded.

The analysis has concentrated on track properties for time intervals referenced to decision time, that is, the time at which a decision to seed or not to seed, was taken. This approach has proved more powerful than considering the properties for the entire storm lifetime, since a physically plausible chain of events has emerged which follows the seeding in a logical sequence that appears to lead to more radar-observed rainfall 20 to 40 minutes after seeding.

The storm track analyses were carried out over the following time periods, 0 being decision time :

-10 to 0
0 to 10
0 to 20
0 to 30
0 to 40 min

a. Elimination of spurious statistical responses

One of the problems that arises when analysing so many variables is that several of them will, by chance alone, reach assigned levels of statistical significance. For example, when analysing 250 track properties, it is probable that 25 will have p values that equal or exceed 90 percent. An exercise that mitigates against reaching erroneous conclusions drawn from chance statistical significances follows. Track properties that reach a certain level of significance should repeat this performance in a subsequent season if the response is real. Re-randomization was therefore performed on the case tracks for each season:

1984/85 - 15 seed, 20 no-seed
1985/86 - 17 seed, 17 no-seed

The scatter plot for the 147 track properties analysed (see Table 3.1) is shown in Fig. 3.8.0. It was decided to choose only those response variables that :

- equal or exceed 90 percent (equal or are less than 10 percent) in the combined seasons analysis
- equal or exceed 70 percent (equal or are less than 30 percent) in each of the separate season analyses.

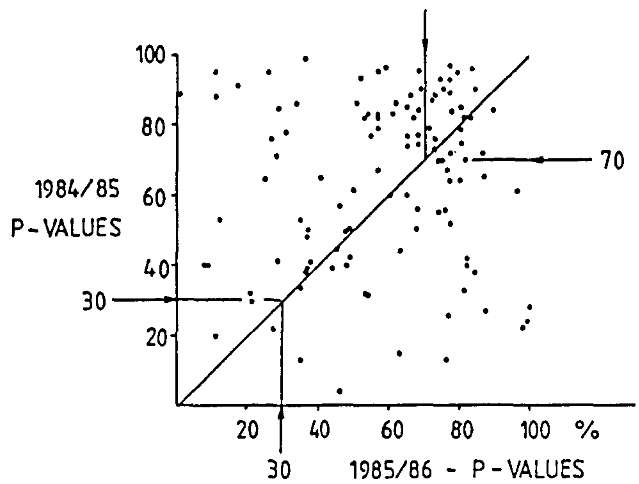

Fig. 3.8.0. Scatter plot of p values computed for the 1984/85 and 1985/86 experimental seasons.

The track properties so chosen are listed in Table 3.2. Some definitions are required to understand some of the listed storm properties.

MROI - maximum rates of increase during the time periods analysed
MROD - maximum rates of decrease

Persistence - a statistic suggested by Tsonis et al., 1983, which has the virtues of being constrained between -1 and 1 and of normalizing the track property being considered.

```
**********************
1. GEOMETRY,TIME 1-10
*********************

- 1    DURATION
- 2    TIME OF ORIGIN
- 3    SPEED OF MOVEMENT
- 4    DIRECTION OF MOVEMENT
- 5    MEAN X CO-ORD
- 6    MEAN Y CO-ORD
- 7    MEAN RANGE
- 8    ENVELOPE DECISION TIME
- 9    VOLUME AT DECISION TIME
- 10   PEAK DBZ AT DECISION TIME

*******************************
2. TOP,DEPTH,VOLUME,MASS 11-48
*******************************

- 11   ECHO TOP - MAX
- 12   ECHO TOP - MAX RATE OF INCREASE
- 13   ECHO TOP - MEAN
- 16   ECHO TOP - PERSISTENCE
- 17   ECHO TOP - MAX RATIO

- 18   DEPTH - MAX
- 19   DEPTH - MAX RATE OF INCREASE
- 20   DEPTH - MEAN
- 23   DEPTH - PERSISTENCE
- 24   DEPTH - MAX RATIO

- 25   VOLUME - MAX
- 26   VOLUME - MAX RATE OF INCREASE
- 27   VOLUME - TIME INTEGRAL
- 28   VOLUME - MEAN
- 31   VOLUME - PERSISTENCE
- 32   VOLUME - MAX RATIO

- 33   MASS TOT - MAX
- 34   MASS TOT - MAX RATE OF INCREASE
- 35   MASS TOT - TIME INTEGRAL
- 36   MASS TOT - MEAN
- 39   MASS TOT - PERSISTENCE
- 40   MASS TOT - MAX RATIO

- 41   MASS A.C.- MAX
- 42   MASS A.C.- MAX RATE OF INCREASE
- 43   MASS A.C.- TIME INTEGRAL
- 44   MASS A.C.- MEAN
- 47   MASS A.C.- PERSISTENCE
- 48   MASS A.C.- MAX RATIO

********************************************
3. AREA,RAIN FLUX,PRECIP WATER,RATIOS 49-92
********************************************

- 49   AREA 3 DEG - MAX
- 50   AREA 3 DEG - MAX RATE OF INCREASE
- 51   AREA 3 DEG - TIME INTEGRAL
- 52   AREA 3 DEG - MEAN
- 55   AREA 3 DEG - PERSISTENCE
- 56   AREA 3 DEG - MAX RATIO

- 57   AREA CUTOFF - MAX
- 58   AREA CUTOFF - MAX RATE OF INCREASE
- 59   AREA CUTOFF - TIME INTEGRAL
- 60   AREA CUTOFF - MEAN
- 63   AREA CUTOFF - PERSISTENCE
- 64   AREA CUTOFF - MAX RATIO

- 65   RFLUX 3 DEG - MAX
- 66   RFLUX 3 DEG - MAX RATE OF INCREASE
- 67   RFLUX 3 DEG - MASS
- 68   RFLUX 3 DEG - MEAN
- 71   RFLUX 3 DEG - PERSISTENCE
- 72   RFLUX 3 DEG - MAX RATIO

- 73   RFLUX CUTOFF - MAX
- 74   RFLUX CUTOFF - MAX RATE OF INCREASE
- 75   RFLUX CUTOFF - MASS
- 76   RFLUX CUTOFF - MEAN
- 79   RFLUX CUTOFF - PERSISTENCE
- 80   RFLUX CUTOFF - MAX RATIO

- 81   PRECIP WATER - MAX
- 82   PRECIP WATER - MAX RATE OF INCREASE
- 83   PRECIP WATER - TIME INTEGRAL
- 84   PRECIP WATER - MEAN
- 87   PRECIP WATER - PERSISTENCE
- 88   PRECIP WATER - MAX RATIO

- 89   MTI/RAIN MASS - 3 DEG
- 90   MTI/RAIN MASS - CUTOFF
- 91   MEAN MASS/RAIN MASS - 3 DEG
- 92   MEAN MASS/RAIN MASS - CUTOFF

*****************************
4. VERTICAL CENTROIDS 93-113
*****************************

- 93   VERT CENTROID - MAX
- 94   VERT CENTROID - MAX RATE OF INCREASE
- 95   VERT CENTROID - MEAN
- 98   VERT CENTROID - PERSISTENCE
- 99   VERT CENTROID - MAX RATIO

- 100 Z-WT VERT CENT - MAX
- 101 Z-WT VERT CENT - MAX RATE OF INCREASE
- 102 Z-WT VERT CENT - MEAN
- 105 Z-WT VERT CENT - PERSISTENCE
- 106 Z-WT VERT CENT - MAX RATIO

- 107 DELT VERT CENT - MAX
- 108 DELT VERT CENT - MAX RATE OF INCREASE
- 109 DELT VERT CENT - MEAN
- 112 DELT VERT CENT - PERSISTENCE
- 113 DELT VERT CENT - MAX RATIO

**********************
6. REFLECTIVITY 119-160
**********************

- 119 PEAK DBZ TOT - MAX
- 120 PEAK DBZ TOT - MAX ROI
- 121 PEAK DBZ TOT - MEAN
- 124 PEAK DBZ TOT - PERSISTENCE
- 125 PEAK DBZ TOT - MAX RATIO
```

Table 3.1 p values were computed for the differences in the seeded and the unseeded means of the above 147 track properties for the 1984/85 and 85/86 seasons and plotted in Fig. 3.8.0.

```
- 126 MEAN DBZ TOT - MAX
- 127 MEAN DBZ TOT - MAX ROI
- 128 MEAN DBZ TOT - MEAN
- 131 MEAN DBZ TOT - PERSISTENCE
- 132 MEAN DBZ TOT - MAX RATIO

- 133 MEAN DBZ 3 DEG - MAX
- 134 MEAN DBZ 3 DEG - MAX ROI
- 135 MEAN DBZ 3 DEG - MEAN
- 138 MEAN DBZ 3 DEG - PERSISTENCE
- 139 MEAN DBZ 3 DEG - MAX RATIO

- 140 MEAN DBZ CUTOFF - MAX
- 141 MEAN DBZ CUTOFF - MAX ROI
- 142 MEAN DBZ CUTOFF - MEAN
- 145 MEAN DBZ CUTOFF - PERSISTENCE
- 146 MEAN DBZ CUTOFF - MAX RATIO

- 147 MAX HT 45'S - MAX
- 148 MAX HT 45'S - MAX ROI
- 149 MAX HT 45'S - MEAN
- 152 MAX HT 45'S - PERSISTENCE
- 153 MAX HT 45'S - MAX RATIO

- 154 HT PEAK DBZ - MAX
- 155 HT PEAK DBZ - MAX ROI
- 156 HT PEAK DBZ - MEAN
- 159 HT PEAK DBZ - PERSISTENCE
- 160 HT PEAK DBZ - MAX RATIO

**********************
7. MASS=f(HT) 161-180
**********************

- 161 MASS=f(HT)  : MEAN - MEAN
- 162 MASS=f(HT)  : MEAN - MAX
- 163 MASS=f(HT)  : MEAN - MIN
- 164 MASS=f(HT)  : MEAN - MAX ROI
- 165 MASS=f(HT)  : MEAN - MAX ROD

*********************
8. DBZ=f(HT) 181-200
*********************

- 181 DBZ=f(HT)   : MEAN - MEAN
- 182 DBZ=f(HT)   : MEAN - MAX
- 183 DBZ=f(HT)   : MEAN - MIN
- 184 DBZ=f(HT)   : MEAN - MAX ROI
- 185 DBZ=f(HT)   : MEAN - MAX ROD

***********************
9. %VOL=f(DBZ) 201-220
***********************

- 201 %VOL=f(DBZ) : MEAN - MEAN
- 202 %VOL=f(DBZ) : MEAN - MAX
- 203 %VOL=f(DBZ) : MEAN - MIN
- 204 %VOL=f(DBZ) : MEAN - MAX ROI
- 205 %VOL=f(DBZ) : MEAN - MAX ROD

*************************
10. %AREA=f(DBZ) 221-240
*************************

- 221 %AREA=f(DBZ): MEAN - MEAN
- 222 %AREA=f(DBZ): MEAN - MAX
- 223 %AREA=f(DBZ): MEAN - MIN
- 224 %AREA=f(DBZ): MEAN - MAX ROI
- 225 %AREA=f(DBZ): MEAN - MAX ROD

******************
11. CONTROL 241-250
******************

- 241 AV MIXING RATIO FOR LOWEST 60 MB
- 242 CCL TEMP
- 243 BUOYANCY AT 500 MB
- 244 CCLTEMP/BUOYANCY 500 MB
- 245 # OF TRACKS FOR THE DAY
- 246 CUMULATIVE 3 DEG A.T.I. FOR THE DAY
- 247 MAX VOLUME OF ANY STORM FOR THE DAY
- 248 MAX RATE OF INCR OF VOLUME OF ANY STORM
- 249 MAX TOPS OF ANY STORM FOR THE DAY
- 250 MAX DBZ OF ANY STORM FOR THE DAY

**********************************************
```

Table 3.1 Continued

Table 3.2 p values for track properties, seasons 1984/85 and 1985/86 combined.

PROP NO	PROPERTY	84/85	85/86	COMBINED
	0 - 30 minutes			
3	Translation speed	92	78	93
32	Volume - Max Ratio	79	81	91
40	Mass - Max ratio	87	80	93
50	3^o Area - MROI	88	75	92
56	3^o Area - Max Ratio	88	75	91
65	Rain Flux - Max	85	80	93
66	- MROI	93	75	91
71	- Persistence	85	80	93
72	- Max Ratio	91	87	93
81	Precip. H_2O - Max	84	82	93
82	- MROI	83	79	91
88	- Max Ratio	89	78	93
119	Reflectivity - Max	91	78	95
121	Reflectivity - Mean	92	78	96
149	Max Ht 45 dBz - Mean	79	88	94
155	Ht Zmax - MROI	82	97	98
164	Mass = f(Ht) - MROI	71	99	99
165	Mass = f(Ht) - MROD	94	90	97

* THOSE TRACK PROPERTIES THAT CORRELATE AT BETTER THAN 0.9

Specifically if:

P_o = value of track property at decision time

P_t = value of track property at time t

Max (P_t,P_o)= either P_t or P_o whichever is the largest

$$\text{Persistence} = \frac{P_t - P_o}{\text{Max }(P_t,P_o)}$$

Max Ratio - this is a variation of the persistence statistic

P_o = value of the track property at decision time

P_m = maximum value reached by that property in the time window being considered

$$\text{Max Ratio} = \frac{P_m - P_o}{P_m}$$

This statistic ranges between 0 and 1 and appears to be very sensitive to changes in track properties. Again, normalization of the track property being considered is achieved by dividing by P_m.

Fig. 3.8.1 displays the p value histograms for each of the seasons and the combined analysis. It is satisfying to see the distribution shift markedly to the right (more properties with higher statistical significance) when the data from the 2 seasons are combined.

b. Changes in radar-measured storm properties with time

One of the methods used to screen the data for biases was to examine track responses over the 10 minutes prior to decision time. Fig. 3.8.2 depicts histograms of 147 track properties analysed, for the time windows shown (decision time = 0). A uniform distribution, which would lie along the dotted line, is not a bad fit to the data at -10 to 0. For the other periods this is no longer true, with greatest departures from a uniform distribution occurring 20 to 40 minutes after seeding.

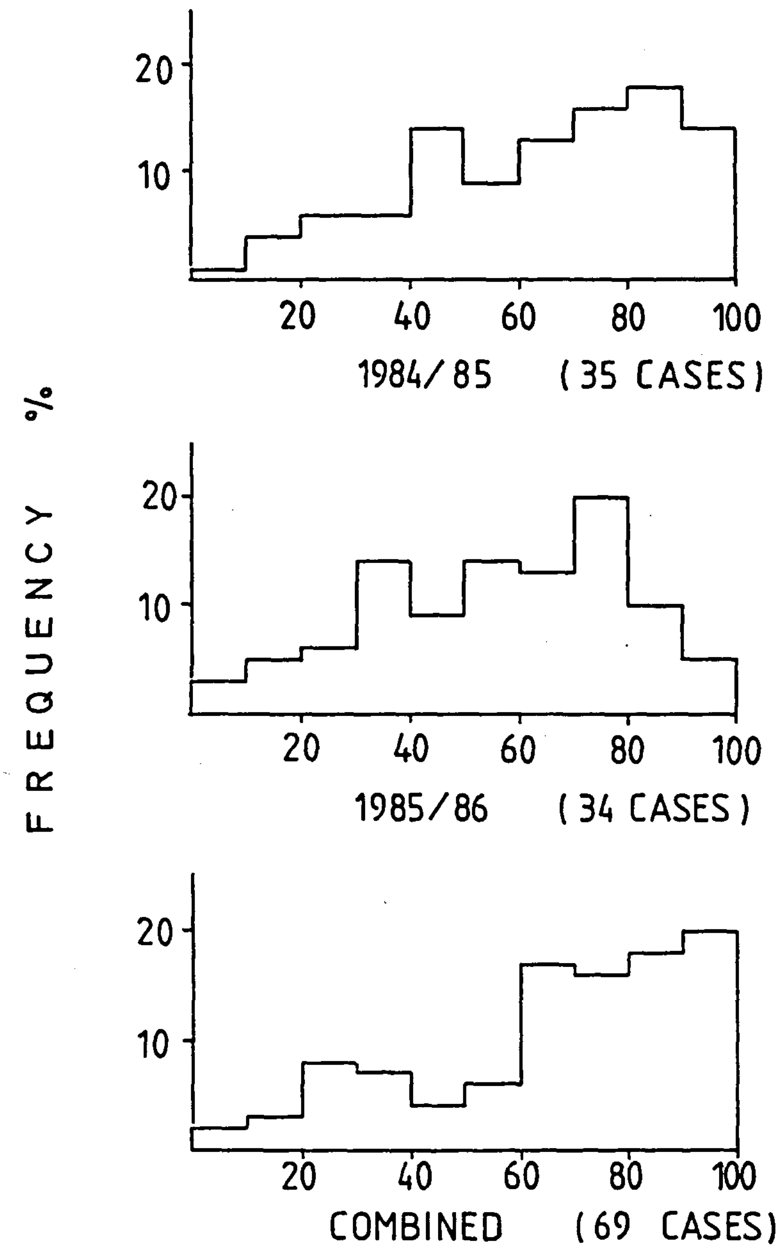

Fig. 3.8.1. Histograms of p values for separate and combined seasons, 0-30 minute time window (147 track properties).

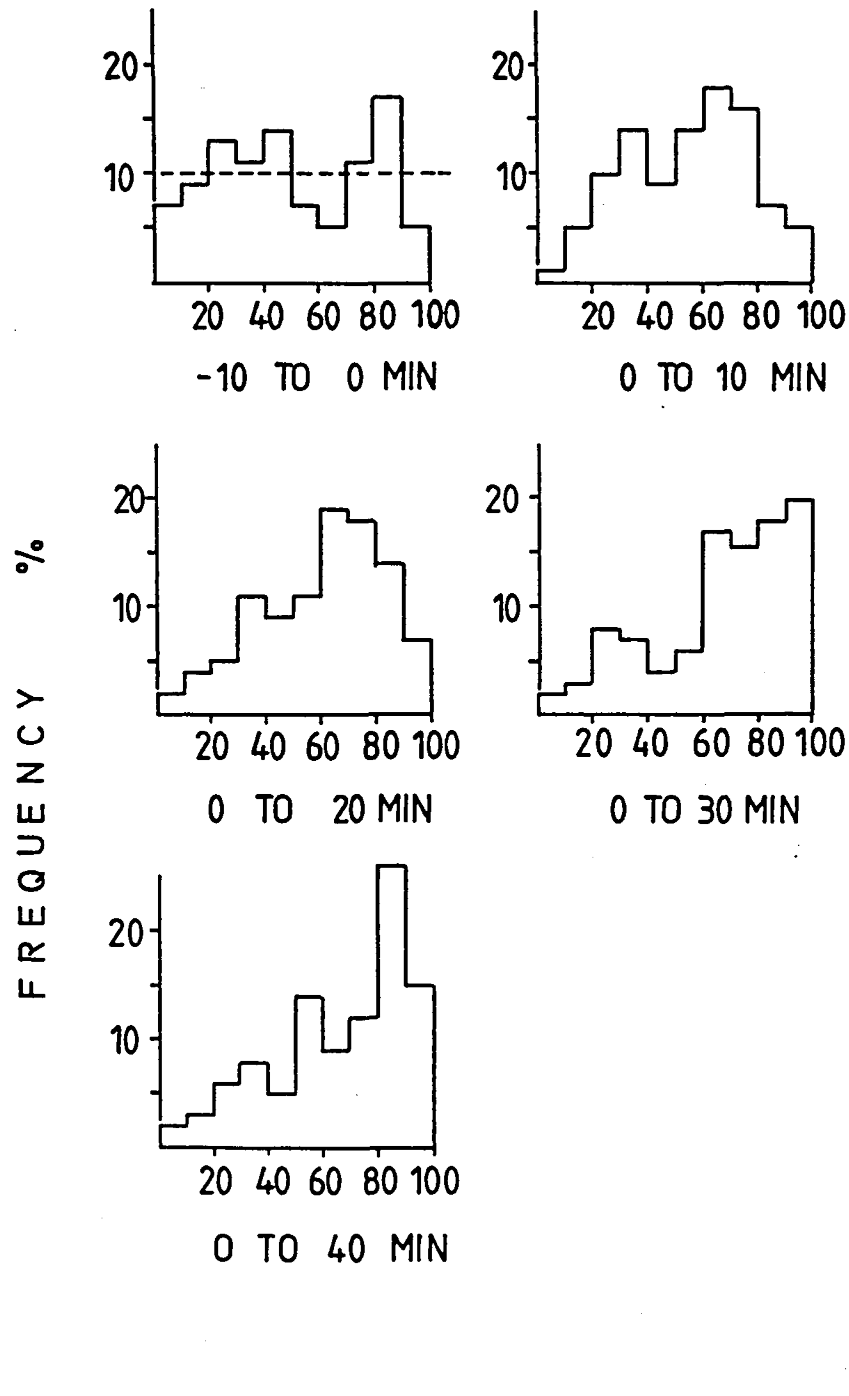

Fig. 3.8.2. Serial histograms of p values for various time windows referenced to decision time (t=0).

Table 3.3 contains probably the most important results from this experiment. As in Table 3.2, only those track properties that score 90 percent or better in the combined seasons analysis and better than 70 percent in each season are considered, but the analysis is applied in each time window (0 to 10, 20, 30 and 40 minutes). Here, the track properties that appear to respond to treatment are listed in serial order.

The first track property seen to respond to treatment is the vertical Volume Centroid (0 to 10 min). Next, 0 to 20 minutes, we see the seeded storms exhibiting greater rates of increase in heights of storm mass (properties 106, 155, 160 and 164, all saying the same thing). This is commensurate with :

- increased updrafts bringing more mass aloft OR
- enhancing the rate of growth of precipitation aloft.

Also in this time period, we see the first response at 3 degrees - seeded storms displaying greater maximum rates of increase in rain flux.

The important seed/no-seed differences show up in the 0 to 30 minute analysis. Here rain fluxes, precipitable water, the gross characteristics of storm mass, volume and 3 degree areas are all apparently responding. Many of these responses are seen to persist into the 0 to 40 minute time window. The average values of the persistence statistic for case track properties of seeded and unseeded case tracks whose differences are approaching acceptable limits of statistical significance are plotted in Fig. 3.8.3.

There are several important features of this analysis that we would like to underline:

a. Biases in the analysis have been guarded against by examining these track properties prior to decision time (-10 to 0 min).

b. The statistical analysis reveals a serial progression of physical events that are completely in accord with plausible seeding hypotheses. None of the events highlighted in Table 3.3 violates physical principles that govern the rates at which such phsyical changes can take place.

c. The responses appear in groups of related track properties.

In the annals of randomized seeding experiments, this is probably the best recorded example of statistical support for a physical hypothesis. In the first 10 minutes after seeding, there is an upward change in the vertical profiles of the seeded storms. This is followed by an apparent increase in the upward rates of mass transport, then a rapid transport of mass downwards which is detected at cloud base (3 degree scan) as an increase in rain flux.

Table 3.3 Calculated percentage changes in seeded track properties with associated p values in parentheses.

PROP NO	PROPERTY	TIME INTERVAL -10 - 0	0 - 10	0 - 20	0 - 30	0 - 40
98	Volume Centroid - Pers.	-30(29)	77(97)	35(85)		
155	Height Zmax - MROI	17(72)		80(100)	62(98)	71(99)
160	Height Zmax - Max Ratio	62(91)		56(93)		
164	Mass = f(Ht) - MROI	-4(44)		116(100)	72(99)	78(100)
108	Vert. Centroid-MROI	17(70)		-24(10)		
66	Rain Flux - MROI	18(69)		48(93)	47(94)	42(94)
65	Rain Flux - Max	39(90)			28(86)	36(93)
71	Rain Flux - Persistence	-14(34)			148(93)	108(90)
72	Rain Flux - Max Ratio	7(61)			43(97)	29(91)
81	Precip. H_2O - Max	59(94)			48(93)	47(93)
82	Precip. H_2O - MROI	16(75)			40(91)	
88	Precip. H_2O - Max ratio	-3(43)			36(93)	
165	Mass = f(Ht) - MROD	-6(45)			43(97)	27(92)
119	Reflectivity - Max	3(91)			4(95)	3(92)
121	Reflectivity - Mean	4(93)			4(96)	4(97)
149	Max Ht 45 dBz - Mean	7(76)			20(94)	26(96)
152	Max Ht 45 dBz-Persis.	-4(42)				50(94)
32	Volume - Max Ratio	-9(30)			30(91)	
40	Mass - Max Ratio	-8(31)			36(93)	30(91)
50	3^o Area - MROI	9(61)			36(92)	
56	3^o Area - Max Ratio	7(61)			28(91)	

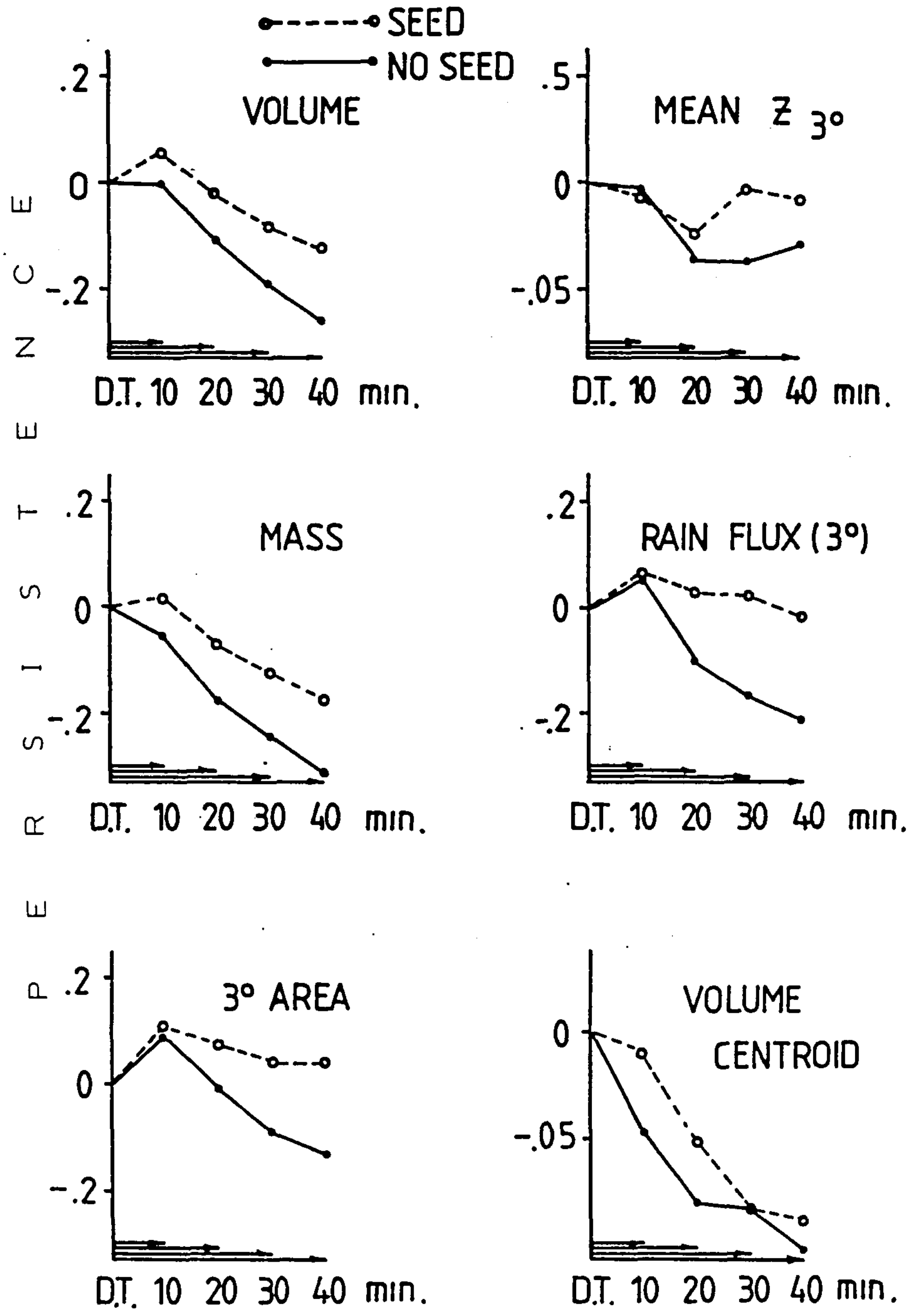

Fig. 3.8.3. Variation of the persistence statistic with time, seed versus no-seed.

3.9 Towards a confirmatory experiment

It is clear that classical statistical significance will be a long time coming if we continue to use 147 track properties. The time has come to start winnowing our response variables. It was suggested that this should be done with the use of Table 3.2. The track response variables in this table have already responded in two separate experimental seasons. If these same variables were to respond in a third season, a very strong case could be made for statistical significance. It only remains to choose one of the intercorrelated variables. Our selection, then, for variables that will respond in a third exploratory seeding season are listed in Table 3.4.

Table 3.4. Track properties that are expected to respond in a third exploratory seeding season.

Time Interval	Prop No	Property
0 - 10	98	Volume centroid-persistence
0 - 20	66	Rain flux - MROI
	155	Zmax Ht - MROI
	160	Zmax Ht - Max Ratio
	164	Mass = f(Ht) - MROI
0 - 30	32	Volume - Max Ratio
	50	3^{0} Area - MROI
	65	Rain flux - Max
	66	Rain flux - MROI
	71	Rain flux - Persistence
	72	Rain flux - Max Ratio
	121	Zmax - Mean
	149	Max Ht. 45 dBz - Mean
	155	Zmax Ht - MROI
	164	Mass = f(Ht) - MROI
	165	Mass = f(Ht) - MROD

This amounts to declaring an inhouse confirmatory experiment, an exercise which is not at odds with the results obtained to date.

We will not only be attempting to forecast the changes in track properties that will occur after seeding, we will also be trying to forecast the time slots into which they will fall. Intuitively, this should increase the statistical power of an experiment. The possibility of designing a statistical test incorporating the time dependence of selected variables for a future confirmatory experiment will be examined by statisticians associated with the programme.

The seeding experiment has been designed to detect those radar-derived variables that appear to be most sensitive to treatment, since possible follow-on experiments, confirmatory in the Nelspruit area and exploratory in other areas, should be as efficient (short) as possible. However, the gross storm characteristics should not be ignored in this exercise. These, while not yet statistically significant, are listed below:

Table 3.5 Increases in seed versus no-seed gross storm properties.

Track Property (0-40 mins)	Increase (%)	p value (%)
Storm volume	29	76
Storm area	23	74
Rain volume	44	89

4.0. THE SEARCH FOR COVARIATES OR PREDICTORS

4.1. The role of predictors in weather modification

Natural rain systems, clouds, behave in a highly variable and erratic way. Their growth or decay is determined by a number of influences, large and small, interacting in nearly unpredictable ways. If we select at random a number of clouds and then simply watch each one for a period of time, some will grow and some will decay; there will be a statistical distribution of cloud behaviours.

This is because they encounter varying forces due to terrain, surrounding wind flow, other cloud, and other (perhaps unknown) influences.

If we then begin operating on these selected clouds with a cloud seeding technology which is truly effective under optimum conditions, their behaviours will still exhibit variability because of the chance interaction of the perhaps unmeasurable forces which drive them. If a cloud is seeded the moment it comes under powerful forces favouring its decay, it will most likely decay.

If the forces dominating the behaviour of a cloud fell within our measurement capability it would be possible to make a prediction of each case and compare its actual behaviour to that predicted. In that condition very few replications of a treatment would be required to evaluate its effectiveness.

Unfortunately, this is not the state of our knowledge concerning cloud behaviour. This forces us into the strategy of randomization, which carries with it great increases in cost and time. This is the reason for current interest in short-term predictors of cloud behaviour - economics - economy in the testing of cloud seeding technology.

With randomization techniques the number of replications of a treatment required to detect an effect is dictated by the size of the expected effect (signal) and by the natural variability (noise) within which it is to be detected. Predictors would reduce the noise by allowing us to measure departures from predicted values rather than the full spectrum of variations.

The difficulties encountered in the search for predictors are formidable. One must know just what parameters and scales are the important ones and then design measurement systems which are adequate to the task. At the present moment we do not know which are the important parameters and hence cannot design and deploy adequate systems.

During the PAWS project we have taken some tentative steps towards the development of predictors using data acquired at smaller scales than the conventional synoptic scale. One of these attempts required the installation of a 9-station network with roughly a 50 km separation between stations for estimating meso-scale convergence and divergence. The other involved the development of a mathematical model to calculate the divergence and convergence generated by rainfall (estimated from the radar data), and using the environmental wind flow (estimated from the sounding).

The model studies, at the time of reporting, are still in the developmental and feasibility stages. They cannot yet bear directly on our primary goal of estimating the potential for rainfall augmentation along the Escarpment region, but are reported on in detail in Vol. IV section 5.2 and 5.3.

Several studies have, however, led to the development of useful predictors. These are:

a. a prediction of the occurrence of large drops at the -10^{o} level in clouds, from environmental sounding parameters

b. a prediction of radar estimated rainfall from unseeded storm populations, using the 30 dBz area-time-integral

These will be described in the following sections.

4.2 Prediction of cloud microphysical characteristics from environmental parameters (Mather, Morrison and Morgan)

The PAWS group has met with very satisfying success in determining the environmental parameters which exert the greatest influence on determining the state of cloud coalescence at the $-10^{o}C$ level in new turrets (Mather et al., 1986).

Most of the cloud sampling has been focussed around the $-10^{o}C$ level since this is the level that is being targetted for glaciogenic seeding. These measurements frequently show the presence of large supercooled water drops implying that the condensation-coalescence mechanism often plays an important role in the local precipitation formation processes.

Dynamic seeding is an attempt to invigorate cloud growth by suddenly releasing large amounts of latent heat. Studies indicate that significant heat release may depend on the presence of large supercooled water drops (Lamb et al., 1981). Several studies (MacCready et al., 1957; Nelson, 1979; Knight, 1981; Johnson, 1982) have suggested that cloud base temperature is a good indicator of whether ice crystals or large water drops will be the dominant graupel embryos in convective clouds. Other factors are liquid water content, air mass of origin (cloud base droplet spectra) and updraft speed. Attempts to relate an active coalescence process to local airmass types in the PAWS experimental area have not been successful using synoptic analyses. More promising is a relationship found between the presence of large drops around the $-10^{o}C$ level and temperatures at cloud base and some measure of updraft potential. This suggests that cloud thermodynamics may be the predominant control over cloud microphysics in this area.

4.2.1 Data

The microphysical data used in this study were obtained from a Particle Measuring System (PMS) Forward Scattering Spectrometer Probe (FSSP) and a PMS 2-dimensional cloud particle imaging probe (2D-C). The FSSP measures the size distribution and concentration of cloud droplets from 2 to 47 microns. Corrections for electronic dead time and variable velocity acceptance ratio (Baugardner and Dye, 1982) have been applied to the FSSP data. The 2D-C probe produces shadow images of cloud particles larger than about 35 microns at a resolution of 35 microns. These data are processed to obtain information on particle concentrations and sizes using the particle weighting technique and standard artifact rejection procedures (Cooper, 1978; Heymsfield and Baugardner, 1985). Smooth circular images with diameters greater than 300 microns encountered at $-10^{o}C$ provide unambiguous evidence of large water drops produced by a condensation-coalescence mechanism (Fig. 4.2.0). Very smooth, round but clearly rimed particles are often observed indicating the birth of graupel as frozen large drops. These too, could be taken as evidence of the importance of coalescence, but have not been considered in this note.

Fig. 4.2.0. Images recorded with 2D-C probe on 7 February 1986. Vertical dimensions of image frame is 1.12 mm.

Cloud base temperatures are determined from the points at which the average equivalent potential temperatures in the lowest 60 mb layer intersect the lines of average mixing ratios for the same layer. The distribution of cloud base temperatures for convective storms in the Nelspruit area is shown in Fig. 4.2.1. On average, cloud base temperatures at Nelspruit are colder than those in Florida and the Midwest, but considerably warmer than those found in the Great Plains (Johnson, 1982).

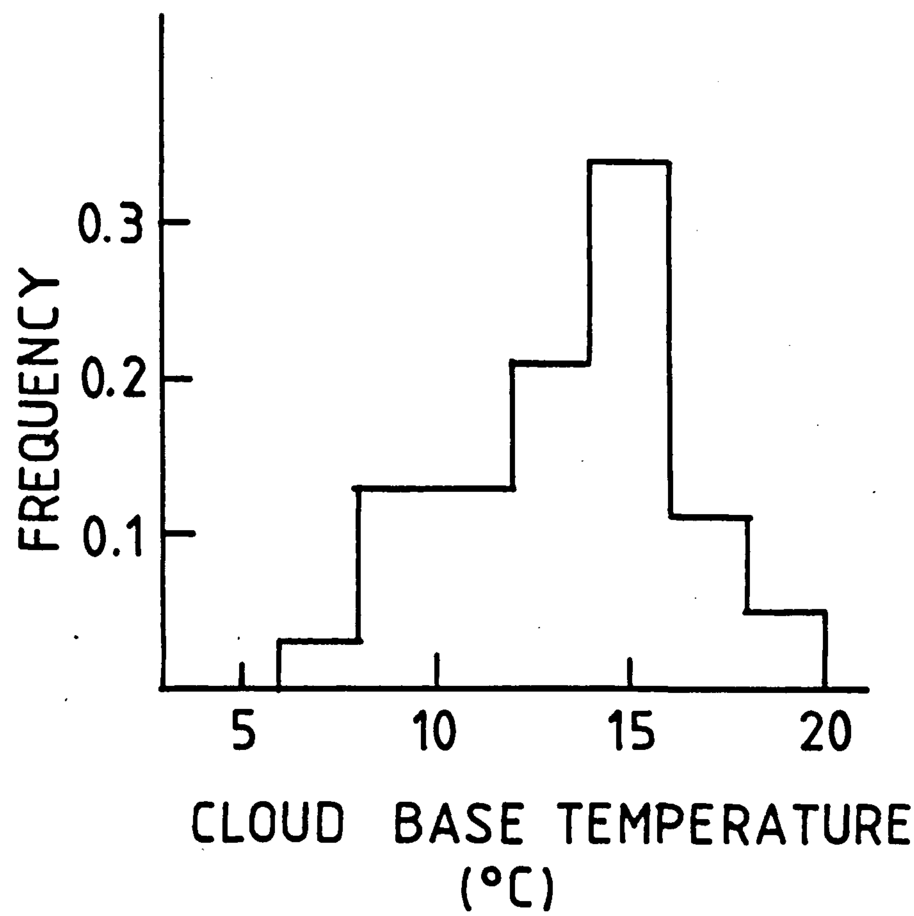

Fig. 4.2.1. Frequency distribution of cloud base temperatures (CBT) computed from 38 Learjet soundings close in time and space to sampled storms.

Measurements from first passes made within 1000 m of the tops of unseeded turrets growing on the flanks of 42 convective storms have been arithmetically averaged for each storm. Only those passes that commenced in environmental air between -8 and -12°C inclusive are considered in this sample. These measurements are summarized in Table 4.1. The numbers in Table 4.1 are storm-averaged 2D-C concentrations of particles whose diameters exceed 105 microns. The numbers in parentheses indicate those storms where clear images of drops greater than 300 microns were found. There is a greater frequency of observed water drops as the FSSP concentrations decrease and mass-weighted mean diameters increase (towards the upper right corner of Table 4.1). Another way of saying the same thing is the more 'maritime' the FSSP spectra around -10° C, the greater the likelihood of observing coalescence-grown water drops. (This follows the tradition of using the terms 'maritime' and 'continental' to describe relative degrees of colloidal instability in clouds). Calculations reported by Young (1974) indicate a rapid decrease in the number of cloud droplets with the onset of coalescence. This opens the question: how much of the observed 'maritime' appearance of the droplet spectra at -10° C is caused by the coalescence? It can be informally reported that, in general, the FSSP measured droplet concentrations at Nelspruit decrease with height on a given flight, sometimes quite dramatically.

Table 4.1. Storm averaged 2D-C particle concentrations (per litre) greater than 105 microns versus averaged FSSP concentrations and mass-weighted mean diameters. Numbers in the table in parentheses are those in which clear images of water drops are recorded.

	Mass-weighted mean diameters (microns)					
Conc. (cm^{-3})	16-17.9	18-19.9	20-21.9	22-23.9	24-25.9	
170-199				10	(13)	
200-229			(4)	(6),(8)	(18)	
230-259			(13)	(18)		
260-289	2		0	(7),(5),(8)		
290-319		0,0,0	(1)	9 (4),(5)		
320-349	3		0,0,0,2	0,1,(4),1,(11),0		
350-379		0,2	4			
380-419		0,1,0		4		
420-449		0,(8)				
450-479		2,1				
Total	2	12	9	17	2	42
Frequency	0.05	0.29	0.21	0.40	0.05	1.0

Imaging probe data cannot discriminate unambiguously between ice crystals and frozen drops or graupel cores. We are tackling this measurement problem at Nelspruit by measuring graupel reflectivities using the on-board aircraft X-band radar and comparing these with reflectivities calculated from the 2D-C probe for various density assumptions (Vol. IV). Care must be taken here to stay within the 2D-C size range (35 - 1120 microns). There is also a big disparity between the sample volumes of the 2D-C probe (about 10 l sec^{-1}) and the radar (5×10^6 m^3 sec^{-1}). Keeping these two caveats in mind, some surprisingly good results are emerging from these comparisons. Indications are that most of the graupel that we are seeing in the high liquid water content cloud regions have densities that are compatable with large frozen drop cores.

Fig. 4.2.2 shows a plot of the temperatures at the convective condensation levels (T_{ccl}) versus the temperature differences between the environmental soundings and the psuedoadiabats (ΔT_{500}) drawn through the CCL for Learjet soundings taken close in time and space to the sampled storms. Each circle in Fig. 4.2.2 represents a storm in which clear images of drops were encountered on at least some of the first passes through turrets rising on their flanks. These drop images were often accompanied by round graupel images. Each cross represents a storm in which only graupel images were gathered by the 2D-C.

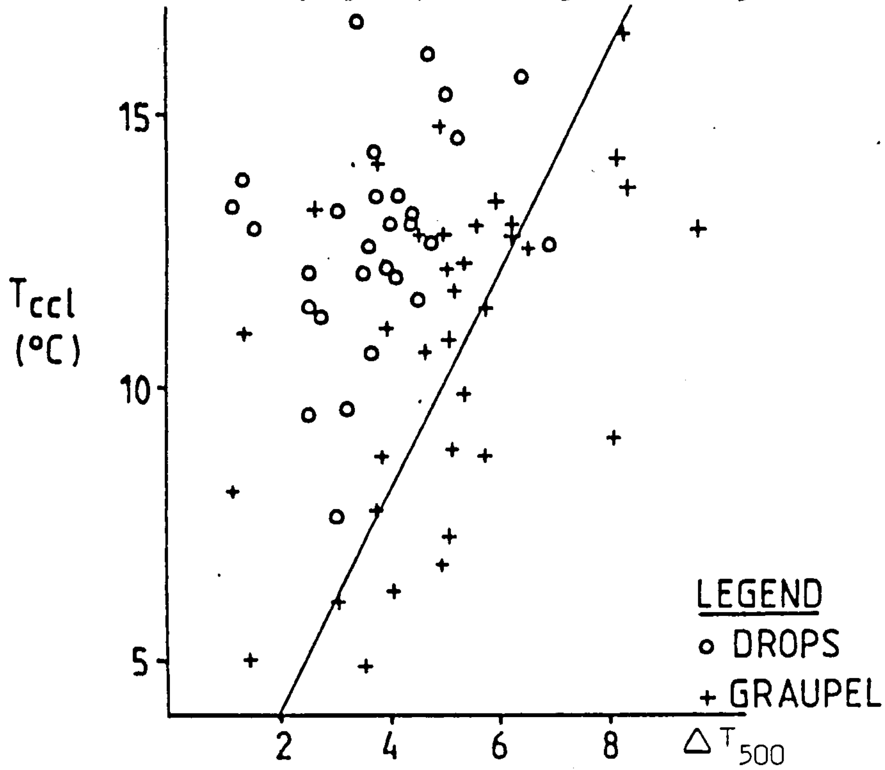

Fig. 4.2.2. Plot of T_{ccl} versus ΔT_{500}. Open circles indicate those storms in which drops plus graupel were encountered. The crosses represent those storms in which only images of graupel were encountered.

4.2.2 Discussion

It is unlikely that the supercooled drops observed at around -10^{o} C are a result of the recycling and melting of ice particles, for at least two reasons. Such a mechanism would tend to produce random observations of drops which could not be related in any systematic way to cloud thermodynamics and other cloud physics observation. Secondly, drops have been observed in isolated cumulus cloud towers on days when they also have appeared in cloud turrets on the flanks of convective storms.

Since T_{ccl} is related to the distance between cloud base and the -10^{o} C level, the ratio T_{ccl}/Delta T_{500} is proportional to the time it takes for a parcel to ascend to the sampling level from cloud base. Since coalescence is a time-dependent process (Leighton and Rodgers, 1974) the speed of rise of an air parcel should also be an important variable in the prediction of the occurrence of large supercooled drops, as well as the cloud base temperature.

Many of the sampled clouds show a mixture of drop and round graupel images. We believe that the round graupel originates from drops that freeze at levels below aircraft penetration level. Indeed some of the clouds that fall into the 'drop' region in Fig. 4.2.2 exhibit only images of round graupel. Pristine images of ice crystals (columns, plates, dendrites, etc.) are only seen occasionally in the relatively 'dead' regions at the edge of clouds, never in the high liquid water regions that are sampled by the Learjet. Any ice crystals nucleated in these regions would almost immediately come in contact with a water drop. The prediction of the formation of ice in cumulus clouds remains one of the most important problems in cloud physics and weather modification.

If dynamic seeding is dependent on the water contained in the large supercooled drops found at glaciogenic seeding levels (Lamb et al., 1981) then a 'coalescence window' may exist for effective dynamic seeding: too large a T_{ccl}/Delta T_{500} ratio and drops will have grown to such a size that they will overcome a relatively weak updraft and fall out of the cloud before reaching sub-zero temperature levels; too small a ratio and the time in the cloud will be too short for coalescence to become significant before the cloud air parcel reaches the level where natural ice nucleation becomes important.

Since coalescence is also dependent upon liquid water content, any entrainment would delay the onset of coalescence (Leighton and Pissimanis, 1975) so best seeding opportunities might be found in those clouds with unentrained cores. Measurements at Nelspruit indicate that cloud turrets rising on the flanks of multicell convective storms often exhibit such unentrained updraft cores. If the storms in Table 4.1 are a representative sample from the population of large convective Nelspruit clouds, then at least 43 percent of the clouds in the area are likely to have an active coalescence mechanism contributing to the precipitation formation processes (those with number concentrations less than 350 cm^{-3} and mass-weighted diameters greater than 22 microns at the -10^{o} C level).

4.3 A radar covariate; A basis for an area experiment (Mather and Prof. Francois Steffans (UNISA))

4.3.1. Introduction

Studies show that probably the biggest impediment confronting an area-wide rain augmentation experiment is the high natural rainfall variability. This is particularly true when dealing with rainfall produced largely by convective storms. To design an experiment that will detect a modest rainfall augmentation effect (signal) against this background of natural variability (noise) is a daunting task.

The experimental unit in area experiments is usually the rainfall day. Some measurement of rainfall is required. It is becoming increasingly clear that, at least with convectively produced rainfall, the weather radar must be the primary rainfall measurement instrument (perhaps supplemented with rain gauges). Any feasible rain gauge network does not have the resolution to adequately measure the rainfall from most convective storms.

Initial results from the PAWS rain augmentation experiment suggest a possible path towards the design of an area rain augmentation experiment. If the results are valid, the design could also be adapted for use in drought relief programmes.

4.3.2. Radar-estimated rainfall and the area time integral

All weather modification researchers realize that the identification of concomitant measurements or covariates that predict what would have happened if there had been no seeding, would lead to easier, less expensive and more effective experiments. Making use of effective covariates would reduce the impact of variability enough to allow one experimental day to tell us as much as several days.

One covariate that has been identified in the work at the South Dakota Institute of Atmospheric Sciences (Smith, et. al., 1985) and at Nelspruit is the relationship between area time integral (ATI - km^2.Hr) and radar-measured rain volume or mass (RERV - 10^3 m^3) both measured over the lifetime of the storm.

The rain volume over an area (a) during time (t) is given by

$$\text{RERV} = \int_T \int_A R \, da \, dt \qquad (1)$$

where R is the rain rate.

The area time integral is :

$$ATI = \int_T \int_A da\, dt = \sum_i A_i \Delta t_i \qquad (2)$$

where A_i is the area over which rain was detected during the i th observation period and Delta t_i is the time between observations (Doneaud et. al., 1984).

Comparisons of ATI's and RERV's using the objective storm tracking technique developed at Nelspruit give correlation coefficients of around 0.98 for plots of the log of RERV versus the log of ATI. The relationship can be expressed as :

$$RERV = A\ (ATI)^B \qquad (3)$$

where A is the intercept and B is the slope on the log versus log plots. The RERV and the ATI for all 1985/86 storms tracked by radar producing 1000 cubic metres of rainfall or more are shown in Fig. 4.3.0. For this season, (3) becomes:

$$RERV = 4.64\ (ATI)^{1.15} \qquad (4)$$

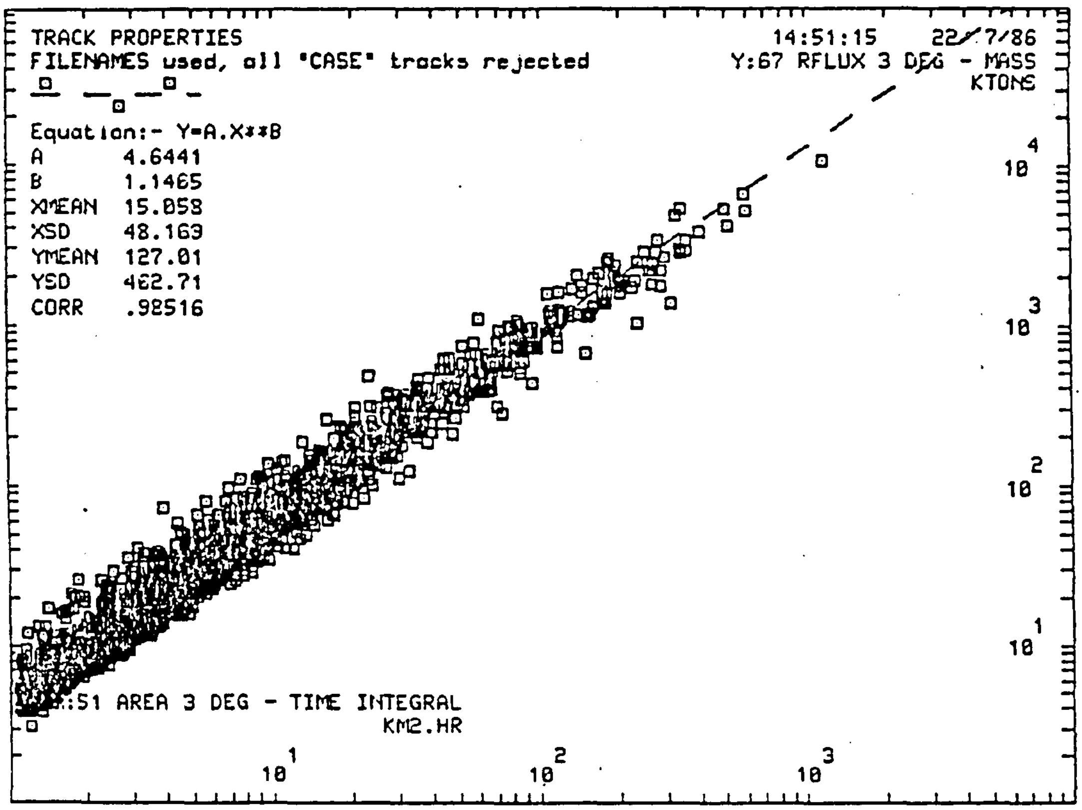

Fig. 4.3.0. Radar estimated rain volumes (RERV) versus area time integrals (ATI) for 1985/86 season. A total of 2599 storm tracks were analysed.

There are slight differences between A and B for the Nelspruit and North Dakota areas. These may be a result of differences in storm tracking schemes or in climates, or a combination of both. The correlation coefficient for (4) is 0.985.

The crucial question is, does (3) change with seeding? If this is the case, then (3) can be used to predict, within fairly narrow limits, what would have happened had seeding NOT taken place. There are indications emerging from the PAWS exploratory rain augmentation experiment that RERV versus ATI does change with seeding.

4.3.3 Results

The approach used here is to analyse all storms (omitting case tracks) on each day that an experiment was performed (either seed or no seed), provided that 15 or more storms were tracked on that day. For each of these days, an RERV versus ATI regression is computed. The ATI for each case track is then used to calculate a predicted rain volume which is compared to the observed rain volume. Table 4.0 lists this analysis for all no-seed tracks and Table 4.1 for the seeded cases.

The relationship between observed rain volume, $RERV_{OBS}$ and the predicted rain volume, $RERV_{PRED}$, was studied and the best fitting relationship turned out to be a log-linear one:

$$\log RERV_{OBS} = 0.1168 + 0.9852 \log RERV_{PRED}$$

which transforms into

$$RERV_{OBS} = 1.124\ RERV_{PRED}^{0.9852}$$

The correlation coefficient between the logarithms is 0.994. The correlation coefficient between the untransformed variables is 0.989, which seems almost as high as the previous correlation. A plot of the residuals of the regression between the untransformed variables reveals that there is a severe heteroskedasticity, the residuals showing a fan shape, indicating increasing variability with increasing predicted response. No such patterns emerge from the residual plots of the log-log regression, and the latter is judged the more appropriate model. There did not appear to be any observable difference in the slopes of the log-log regression lines corresponding to the seeded and unseeded cases, but a plot of the residuals showed a marked difference between the intercepts, indicating a possible seeding effect.

To evaluate the effect of seeding on the observed rain volume, the seeded and unseeded cases were compared with respect to the residuals from the common log-log regression line. The mean difference was 0.115, which is interpreted as the estimated difference between the intercepts, i.e. given two storms with the

Table 4.1 No-Seed Cases.

No	Date	Case No	Storms	A	B	ATI	PRED	OBS
1	30/10/84	5	143	4.32	1.12	4.15	21	20
2	11/11/84	7	17	4.53	1.20	119.51	1409	1268
3	27/11/84	11	36	4.45	1.15	3.86	21	18
4	29/11/84	14	143	4.41	1.10	83.22	571	691
5	12/12/84	18	41	5.40	1.17	113.32	1367	1512
6	13/12/84	19	88	4.70	1.17	14.61	108	101
7	13/12/84	20	88	4.70	1.17	66.90	642	600
8	14/12/84	21	37	4.84	1.11	134.60	1117	1137
9	17/12/84	23	27	5.48	1.18	24.00	233	240
10	18/12/84	24	28	4.56	1.22	30.18	291	289
11	19/12/84	25	51	5.32	1.17	10.73	85	69
12	7/01/85	30	36	4.99	1.19	122.83	1529	1636
13	15/01/85	31	135	5.15	1.16	32.63	293	366
14	18/01/85	34	115	4.84	1.17	29.14	250	261
15	7/02/85	38	52	5.81	1.12	43.32	396	371
16	16/02/85	37	36	4.64	1.08	7.08	38	48
17	1/03/85	43	62	5.70	1.18	169.45	2433	1955
18	1/03/85	45	62	5.70	1.18	35.63	386	346
19	13/03/85	48	53	4.67	1.20	7.97	56	50
20	13/03/85	49	53	4.67	1.20	178.39	2349	1720
21	29/10/85	54	70	4.47	1.16	746.24	9613	9396
22	14/12/85	65	105	5.05	1.13	96.94	887	817
23	14/01/86	73	84	4.12	1.19	117.33	1195	1080
24	14/01/86	74	84	4.12	1.19	35.49	288	302
25	15/01/86	76	135	5.15	1.16	12.65	98	84
26	18/01/86	77	92	5.38	1.11	3.01	18	18
27	29/01/86	78	91	5.39	1.12	14.78	110	91
28	5/02/86	80	133	4.29	1.16	38.69	298	396
29	7/02/86	82	131	5.73	1.09	43.66	351	404
30	7/02/86	83	131	5.73	1.09	12.61	91	94
31	22/02/86	93	110	4.62	1.17	37.60	322	306
32	12/03/86	101	37	4.46	1.17	91.65	881	1106
33	13/03/86	102	28	4.86	1.20	80.13	936	649
34	14/03/86	103	75	5.08	1.16	54.53	525	525
35	14/03/86	104	75	5.08	1.16	274.65	3426	3300

Table 4.2 : Seeded Cases.

No	Date	Case	Storms	A	B	ATI	PRED	OBS
1	1/11/84	6	209	5.41	1.14	201.18	2287	3028
2	16/11/84	10	48	5.63	1.22	302.37	5981	7236
3	28/11/84	12	52	4.28	1.22	12.16	90	99
4	29/11/84	13	143	4.41	1.10	99.91	698	701
5	19/12/84	26	51	5.32	1.17	12.82	105	117
6	20/12/84	28	65	5.46	1.18	32.51	332	433
7	15/01/85	32	135	5.15	1.16	34.40	312	321
8	15/01/85	33	135	5.15	1.16	7.16	50	94
9	18/01/85	35	115	4.84	1.17	31.07	270	303
10	23/02/85	40	103	4.76	1.15	134.24	1332	1248
11	28/02/85	41	64	5.19	1.17	63.36	666	783
12	28/02/85	42	64	5.19	1.17	105.80	1213	1084
13	1/03/85	44	62	5.70	1.18	108.20	1433	1101
14	12/03/85	46	50	4.92	1.1[illegible]	[illegible]31	694	765
15	12/03/85	47	50	4.92	1.16	6.44	43	45
16	16/10/85	53	15	5.47	1.19	178.62	2617	2310
17	29/10/85	55	70	4.47	1.16	56.37	480	555
18	2/11/85	56	21	4.67	1.21	84.78	1006	998
19	9/11/85	60	161	4.62	1.13	150.78	1337	1510
20	3/12/85	62	15	5.01	1.15	43.80	387	459
21	3/01/86	68	78	4.57	1.14	4.32	24	19
22	3/01/86	70	78	4.57	1.14	21.95	154	138
23	5/02/86	81	133	4.29	1.16	147.15	1403	1635
24	7/02/86	84	131	5.73	1.09	594.34	6051	6879
25	13/02/86	91	77	5.04	1.08	22.56	146	165
26	3/03/86	95	21	3.96	1.19	2.43	11	14
27	3/03/86	96	21	3.96	1.19	13.50	88	120
28	10/03/86	99	149	4.90	1.15	217.09	2384	2003
29	10/03/86	100	149	4.90	1.15	41.60	356	433
30	14/03/86	105	37	5.08	1.16	69.08	691	699
31	24/03/86	106	147	4.03	1.09	21.26	113	136

same predicted RERV, we estimate that the observed RERV will differ as follows:

$$\log RERV_S - \log RERV_{NS} = 0.115$$

i.e. $$RERV_S = 1.12\ RERV_{NS}$$

where: S = seed
NS = no-seed

A permutation test was used to test the significance of this difference, and the p value was found to be 0.006, i.e. the observed difference was found to be highly significant. The 95% confidence interval, based on the permutation test, using an algorithm developed by Kahn (1986) is as follows:

$$0.032 < \log RERV_S - \log RERV_{NS} < 0.195$$

$$1.03 < \frac{RERV_S}{RERV_{NS}} < 1.22$$

A potential source of bias was found to be the number of storms used in computing the formula for predicted RERV. The slope B (see tables 4.1 and 4.2) was found to be correlated with the number of storms (r=0.5), and due to the luck of the draw, the mean number of storms corresponding to seeded cases (76.7) was substantially lower than the mean number of storms corresponding to unseeded cases (87.6). While this difference is not significant (p value 0.325) such a difference should not be disregarded as a potential source of bias. A further regression analysis was therefore performed, adjusting for the number of storms. The adjusted 95% confidence interval for the ratio of seeded and unseeded rain volumes was found to be (1.026: 1.203) which shows that the number of storms did not unduly affect the outcome.

4.3.4 Discussion

Indications are that for a given 3 degree storm area, seeded storms are raining harder than their untreated counterparts. Several comments are in order here.

a. These results may be diluted by the current experimental design which limits seeding to a total of roughly 120 seconds. Thus, most of the seeded storms will have been treated over only a portion of their total lifetimes.

b. Since, even in an area experiment, it is unlikely that more than 25 percent of the storms will be treated, there will be plenty of "control" storm tracks available from which to calculate predicted rain volumes.

An area experiment using the rain day as the experimental unit would be using "in day controls", thus compensating for any climatic changes either seasonal or long term ("maritime" and "continental" airmasses, wet and dry cycles).

c. With the use of a good radar, the technique could be employed in emergency drought relief efforts. An estimate of the additional rainfall produced would provide a measure of the cost effectiveness of such operations.

d. Results from the randomized experiment suggest that storm areas as well as rain fluxes are increased by seeding, so the rainfall increases estimated by the method outlined above should be conservative. Increases in storm areas for seeded versus unseeded storms could be handled in the normal manner in a randomized experiment. However, many more cases would probably be required to evaluate this effect because of the inherent variability of this statistic.

e. If the above results are valid, an experiment using convective complexes as the experimental unit should detect that seeded storms produce more rainfall per unit area than their untreated counterparts after 50 to 60 trials (at acceptable levels of statistical significance).

f. This excercise shows the power of a good covariate. Even a modest (12%) apparent increase in rainfall required just 66 trials to reach a p value of 0.006.

4.4 Synoptic and large scale effects (Garstang and Emmitt)

Changes in moisture in the troposphere below 6 km are shown in Volume II, Section 4.2 to be the most significant synoptic scale changes visible over the season. Departures in moist static energy have been examined from a diagnostic point of view to determine the synoptic scale conditions under which seeding was carried out. Table 4.3 shows the distribution of seeding and sampling over the 1984/85 and 85/86 seasons corresponding to classes of moist static energy departure at the surface and from the surface to 6 km. Table 4.3 also shows the correspondence of these classes with previously determined mesoscale forcing classes.

There is no correspondence between the departures in moist static energy and the mesoscale classes. This suggests that on the scale of the network the forcing can be either on the synoptic scale or the mesoscale. Strong mesoscale forcing is certainly not confined to days on which there are large moist static energy departures. Thus the effect of synoptic scale forcing might be viewed independently of other scales of forcing.

Examination of the radar response to seeding on days with large and small departures in moist energy shows no significant differences between the static energy environment of the seed and no-seed cases. Evidence to date suggests that discrimination of the magnitude of seeding effects as a function of the synoptic scale forcing is not yet possible. This does not appear to be necessarily true for scales below the synoptic. Both the mesoscales and the convective scales contain interesting (but not statistically significant) indicators of differences in the environments of the seed and no-seed groups.

4.5 Mesoscale and convective scale effects

Differences in the radar responses of the seed and no-seed pools are shown in Section 3.1 to be not only detectable but to follow in a physically logical progression in time up to 40 min beyond initial treatment. Important questions then follow regarding the near (mesoscale and smaller) environments of the seeding targets and the possibility of unlucky randomized draws. Two questions, in particular, are pursued in this section:

a) is there any significant difference between the mesoscale or convective scale environments of the seeded and non-seeded case pools?

b) does forcing (prestorm) on the mesoscale influence the seeding response?

Table 4.3. Synoptic scale forcing. Departures in moist static energy (units J $kg^{-1} \times 10^3$). Only dates on which seeding or sampling were done are included.

Small Negative -6 MSE 0 (green)	MF	Small Positive 0 MSE 6 (yellow)	MF	Large Positive 6 MSE (red)	MF
30 Oct 84	?	27 Nov 84	W	28 Nov 84	W
1 Nov 84	S	29 Nov 84	W	19 Dec 84	?
11 Nov 84	No	4 Jan 85	?	20 Dec 84	?
12 Nov 84	S	23 Feb 85	?	7 Jan 85	?
16 Nov 84	S	12 Mar 85	?	15 Jan 85	?
10 Dec 84	W	16 Oct 85	S	18 Jan 85	?
12 Dec 84	W	3 Dec 85	No	16 Feb 85	?
13 Dec 84	W	11 Feb 86	S	28 Feb 85	?
14 Dec 84	S	12 Feb 86	S	1 Mar 85	?
13 Mar 85	?	10 Mar 86	S	29 Oct 85	S
8 Oct 85	?	12 Mar 86	No	2 Nov 85	No
3 Mar 86	S			7 Nov 85	No
6 Mar 86	No			8 Nov 85	S
24 Mar 86	No			9 Nov 85	S
				26 Nov 85	W
				7 Dec 85	S
				14 Dec 85	S
				3 Jan 86	W
				14 Jan 86	W
				15 Jan 86	S
				18 Jan 86	W
				29 Jan 86	W
				5 Feb 86	W
				7 Feb 86	S
				10 Feb 86	W
				13 Feb 86	No
				22 Feb 86	S
				13 Mar 86	W

MF denotes level of mesoscale forcing where:

S = strong, greater than 1.5×10^{-4} sec^{-1}
W = weak, $.5 - 1.5 \times 10^{-4}$ sec^{-1}
No = none or very weak, less than $.5 \times 10^{-4}$ sec^{-1}
? = no mesoscale data

We first ask questions about the nature of the seed, no-seed and control cases which formed the basis for the seeding signal obtained in Section 3.1. The Area Time Integrals (ATIs) of radar returns at 3^{o} scan angle have been found to be strongly related to the Radar Estimated Rain Volume (RERV). We use the ATI as an indicator of rainfall production. Table 4.4 displays the lifetime ATI signal for 32 seed and 37 no-seed cases. There is no statistically significant difference between the seed and no-seed cases as far as their entire lifetime ATI's are concerned. In Section 3.1 we demonstrated that there are differences in other properties on shorter time scales. It was also noted that the relationship between the ATI and RERV for the seeds was different from that of the no-seeds. Table 4.4 shows that while there may be little difference in the lifetime ATI's of the target cells there is a clear difference between those cells chosen for randomized treatment (seed/no-seed) and those other cells on the same day which have lifetimes greater than 20 minutes. This difference must clearly be considered in any target/control analyses.

Mesoscale forcing has been characterized in terms of the convergence/divergence over the mesoscale meteorological network. In Vol. II, Section 4, a detectable but weak relationship was shown to exist between the mesoscale positive divergence signal and rainfall measured with widely spaced raingauges. Using the radar data and considering only the magnitude of the convergent portion of the mesoscale divergence signal, the lifetime statistics of non-target radar cells occurring on strong vs. weak mesoscale convergent days showed a significant difference in convective activity both in amount (number of cells, ATI) and individual behaviour (max volumes, max rates of increase, max dBz).

In this volume we continue to focus upon the strength of the prestorm convergence and the subsequent radar activity. Table 4.5 summarizes the stratification of the non-target radar cell properties on the basis of the magnitude of the prestorm mesoscale convergence. Since the radar activity appears related to the prestorm mesoscale convergence, then the next question is, how are the seed and no-seed cases distributed between the days classified as strongly or weakly convergent.

Table 4.6 shows 45 days which exhibit an hourly averaged mesoscale convergence greater than 0.2×10^{-4} sec^{-1}. These 45 days are stratified into three groups defined in the table: 15 strong; 13 moderate; 17 weak. On 34 of these days (12 strong; 11 moderate; 11 weak) seeding operations were carried out. On these 34 days there are 27 seeded and 30 no-seed cases. However, only on 28 of these 34 days were cases selected for seeding signal analysis (see Section 3.1). On these 28 days, 17 cases were seeded and 23 cases were not seeded. Therefore the following statements are based upon 40 of the 64 cases meeting the selection criteria. Table 4.7 summarizes these days for strong, moderate, and weak mesoscale prestorm convergence. Random selection results in an extreme class stratification ratio of

Table 4.4. Comparison of ATI(km^2 hr) statistics for seed/no-seed cases selected for seeding signature evaluation.

	Average Target ATI	Average Control* ATI	Daily** Ratio
32 seeds	90(116)	31(20)	3.0(3.1)
37 no-seeds	79(126)	28(11)	2.8(3.0)
p differences	90	90	90

* taken from summary statistics for radar cells persisting longer than 5 radar scans (about 30 minutes) on the same day.

** ratio of target cell ATI to average control cell ATI for the same day.

Numbers in parentheses are the standard deviations.

Table 4.5. Summary of control cell radar statistics on days having seed/no-seed cases used in analysis.

Mesoscale Pre-storm	No of Tracks	ATI	Vol	Rate max	Top max
9 strong	68 (46)	2326 (1228)	2381 (1551)	1.45 (.70)	14605 (1764)
9 moderate	49 (25)	1414 (577)	1507 (920)	1.17 (.58)	14456 (1398)
10 weak	50 (34)	1479 (912)	1491 (1009)	1.12 (.60)	14949 (2385)
p value between strong and weak cases	.81	.94	.91	.83	.38

Definitions : No. of Tracks - number of non-targeted cells identified and tracked by the cell tracking programme for at least 5 radar scans (about 30 min)

ATI - ATI at 3° scan angle for cells counted above accumulated over the whole time the radar is on

Vol_{max} - maximum volume of any of the control cells

$Rate_{max}$ - maximum rate of volume increase between scans for any of the control cells

Top_{max} - maximum top height (km) of any of the control cells

Strong - maximum hourly average divergence less than $-.9 \times 10^{-4}$ sec^{-1}

Moderate - maximum hourly average divergence $-.6$ to $-.8 \times 10^{-4}$ sec^{-1}

Weak - maximum hourly average divergence greater than $-.6 \times 10^{-4}$ sec^{-1}

Table 4.6. Ranked Inventory of the prestorm convergence signal on 45 operation days. Circles indicate data used in overall seed/no-seed analysis (see Vol. III, Section 3.1). Y= seed
N= no-seed

Network refers to boundaries of PAWS 9 station mesoscale network.

a) Strong Mesoscale Prestorm Convergence

Date	Target Location Over Network	Target Location Outside of Network	Network Total Rain (mm)
01 Nov 84	-	Ⓨ	96.2
12 Nov 84	Y	Y	148.0
16 Nov 84	Ⓨ	-	37.8
29 Nov 84	Ⓨ	Ⓝ	96.8
16 Oct 85	Ⓨ	-	2.0
29 Oct 85	Ⓨ	Ⓝ	186.0
08 Nov 85	-	N	45.0
09 NOv 85	-	Ⓨ	122.5
22 Nov 85	-	-	-
07 Dec 85	-	N/Y	14.5
11 Dec 85	-	-	4.0
14 Dec 85	-	Ⓝ/N	2.8
04 Feb 86	-	-	29.5
07 Feb 86	-	Ⓨ Ⓝ Ⓝ	41.5
03 Mar 86	-	Ⓨ Ⓨ	.8

Table 4.6 (cont)

b) Moderate Mesoscale Prestorm Convergence

Date	Target Location Over Network	Target Location Outside of Network	Network Total Rain (mm)
27 Nov 84	Ⓝ	-	63.0
28 Nov 84	Ⓨ	-	101.0
10 Dec 84	-	N/Y	24.2
12 Dec 84	-	Ⓝ	160.2
14 Dec 84	-	Ⓝ Y	46.0
06 Dec 85	-	-	5.2
03 Jan 86	Ⓨ	Ⓨ Y	32.0
18 Jan 86	Ⓝ	-	20.5
05 Feb 86	Ⓨ	Ⓝ	49.2
11 Feb 86	-	Y	75.8
21 Feb 86	-	-	40.0
22 Feb 86	-	N Ⓝ	32.8
13 Mar 86	Ⓝ	-	4.0

Table 4.6. (Cont)

c) Weak Mesoscale Prestorm Convergence

Date	Target Location Over Network	Target Location Outside of Network	Network Total Rain (mm)
13 Dec 84	Ⓝ	Ⓝ	24.2
26 Nov 85	Ⓨ	-	58.5
30 Dec 85	Ⓝ	-	71.8
07 Jan 86	-	Ⓝ	1.2
12 Jan 86	-	-	18.5
13 Jan 86	-	-	49.5
14 Jan 86	Ⓝ	Ⓝ	23.5
15 Jan 86	Ⓝ	Y	38.5
29 Jan 86	Ⓝ	Y	58.0
06 Feb 86	-	-	58.0
08 Feb 86	-	-	24.5
09 Feb 86	-	-	26.2
10 Feb 86	-	-	20.2
12 Feb 86	-	N/Y/N/Y	34.5
10 Mar 86	Ⓨ	Ⓨ	96.5
12 Mar 86	-	Ⓝ	69.8
14 Mar 86	Ⓝ	Ⓝ Ⓨ	12.5

Table 4.7. Distribution of seeding targets on days with strong and weak mesoscale pre-storm convergence.

Mesoscale Forcing Response	Strong	Moderate	Weak	Total
No of days with seeding targets	12	11	11	34
No of days with seeding targets used in analysis	9	9	10	28
Seed Cases	9	4	4	17
No-seed cases	5	7	11	23
Extreme Class Stratification Ratio (see text)		20/9 = 2.22		

20/9 - i.e. the ratio of (seeded storms under strong mesoscale forcing + non-seeded storms under weak mesoscale forcing) to (seeded storms under weak mesoscale forcing + non-seeded storms under strong mesoscale forcing). This stratification ratio may only have meaning to the seeding signal analysis if it can be shown that the natural clouds are different on days with strong vs. weak mesoscale forcing.

Table 4.8 shows that there is a difference in the ATI between groups of target cases which have been independently classified by the mesoscale prestorm convergence signal. The target ATI's include those of both seed and no-seed cases, while none of the control clouds has been targetted. Table 4.8 implies, as far as the ATI statistics are concerned:

Table 4.8. Comparison of target ATI's on days with strong and weak mesoscale signals. Standard deviations are in parentheses.

	Target ATI	Average Control ATI	Average Daily Ratio	p value for Difference between Columns 1 & 2 (all)
Strong (14 cases)				
all	184 (216)	40 (25)	4.6	.99
9 seed	177 (173)			
5 no-seed	197 (276)			
Moderate (11 cases)				
all	54 (52)	31 (10)	1.7	.97
4 seed	46 (59)			
7 no-seed	59 (48)			
Weak (15 cases)				
all	70 (77)	30 (11)	2.3	.97
4 seed	83 (81)			
11 no-seed	66 (74)			
p value for Strong vs. Weak (all)	.96	.91		

a. Days with strong mesoscale pre-storm convergence produce larger and more productive targets than those days with lesser forcing.

b. There is not a significant difference between ATI's in moderate and weak classed days.

c. The target cells on days with strong pre-storm mesoscale forcing are more productive than the non-targetted cells on the same day by a larger ratio (4.6) than for moderate (1.7) or weak (2.3) days.

d. There is no detectable difference in the seed and no-seed cases on the strong days, i.e. seeds as well as no-seeds produce roughly the same ATI over their lifetimes.

This last point (4) addresses question b. above, however, the sample size does not allow any conclusion to be drawn. In general, the seed/no-seed data set is too small (64 cases) to permit more than two or three levels of stratification. Furthermore, similar analyses (now underway) need to be done using those radar properties shown in Tables 3.1 and 3.2.

This effort to document differences in the mesoscale environment of the seeding targets can only suggest that there may be physical differences and therefore caution should be exercised.* At present, however, the mesoscale forcing cannot account for the apparent seeding signal discussed in Section 3.1. For discussion of additional efforts to examine the near environments of the seeding targets the reader is referred to Vol. IV, Section 5, Algorithm Development of Thunderstorm Outflow and Interaction.

* A bad draw is evident in the above limited data set when the re-randomization analysis discussed in Section 3.0 of this report is run on the 17 seed and 23 no-seed cases shown in Table 4.6. It is well to remember that this is just 58 percent of the total number of cases. Addition of the 29 cases not included in the analysis in this section redresses the imbalance in the data set noted above.

5.0 SEEDING OPPORTUNITIES, THE ECONOMIC ASPECT (Mather)

One question that deserves an answer early on in any rainfall augmentation feasibility study is, "How much of the seasonal rainfall do the seedable clouds produce?" One of the main reasons for installing the 16 gauge automatic raingauge network in the Badplaas valley was to provide an answer to this question. The following assumptions were made in this study:

a. Cloud seeding operations can only be conducted during daylight hours (0600-1900 hrs SAST).

b. The "seedable" clouds can be adequately classified by using certain average characteristics that have been obtained from the radar analyses of those storms that were chosen as cases in the randomized experiment.

Table 5.1 lists rainfall statistics from the raingauge network which operates from Oct. 1 through to Mar. 31. The two seasons tabulated indicate, that on average, 59% of the summer season rainfall falls during the day. The rainfall totals listed in the column "during radar ops" were recorded when the radar was operating in volume scan mode. A comparison of the radar-measured rainfall for these periods is listed below (Table 5.2).

Table 5.1 Rainfall statistics from the automatic raingauge network.

SEASON	RAINFALL IN MILLIMETERS				
	Total	Night (19-06)	Day (06-19)	During Radar ops	Day Total (%)
1984/85	594	229	365	98	61
1985/86	586	254	332	134	57

Table 5.2 Comparison of radar and gauge measured rainfall.

	Rainfall estimates		
Season	Gauge network (mm)	Radar (mm)	Radar/Gauge %
1984/85	98	35.5	36
1985/86	134	30.6	23

On average, the radar estimate is only about 30 percent of the rainfall measured by the gauges. This is probably due to :

- the high angle of scan (3 degrees) over the raingauge network
- the partial blocking of the 3 degree radar beam by the terrain in that direction.

The observed average storm track characteristics that best separate the "seedable" from the rest of the storm tracks are :

- maximum echo tops greater than 6400 m (clouds must exceed this level to penetrate the -10°C isotherm) peak reflectivities greater than 40 dBz (see Learjet launch criteria)
- $T_{ccl}/\Delta T_{500} \geq 2.0$ (see Section 4.2)

All selected case tracks equal or exceed the above criteria. The radar records were then searched for all other storms that exceed these 3 criteria.

The radar estimated rainfalls for all storms and "seedable" storms for the past 2 seasons are listed in Table 5.3.

Table 5.3 Estimate of "seedable" rainfall.

	Radar measured rain mass		
Season	All storms (Ktons)	Seedable storms (Ktons)	Seedable storms / All storms %
1984/85	330,225	223,097	68
1985/86	333,630	211,422	63

From the above, roughly 65 percent of all storm tracks are seedable. Assuming only daytime operations, about 38 percent of the total seasonal rainfall is seedable (0.65 x 0.59). If all seedable storms were treated, then increases averaging 40 percent would have to be achieved to obtain seasonal increases in rainfall of around 15 percent.

There are indications that rainfall increases of this order were achieved in some seasons during the 10 years of hail suppression seeding (Gabriel and Mather, 1986). Estimates made during this period suggested that approximately 25 percent of the large storms were seeded. This implies (assuming they were "seedable" storms) that individual storm increases exceeded

100 percent.

This statistic, if valid, will have a profound impact upon the future design of a successful technology. Increases of these magnitudes targetted into catchment areas at specific times could have a significant impact upon run-off.

6.0 THE QUESTION OF TRANSFERABILITY: A PILOT STUDY (Morgan and Wightman)

The PAWS cloud physical and cloud seeding studies have been carried out in a fixed region, the Lowveld escarpment near Nelspruit. It is natural at this time to ask about the transferability of results obtained in that region to other regions. Certainly, every region to be considered will have its own characteristics and a certain amount of field study would be required in each to answer this question.

An important result of the PAWS has been the realization that the microphysical character of Nelspruit clouds (and hence their seedability) is largely determined by dynamical factors (buoyancy, cloud base temperature) rather than by microphysical characteristics of the low level air mass (such as condensation nucleus concentrations), as described in section 5.6.2 of Vol. II of this Final Report and in Mather et al., 1986. This can be made the basis of a preliminary statement on transferability of Nelspruit results to other regions of South Africa.

To the extent that the microphysical characteristics of the clouds of other regions are determined as in Nelspruit (this is neither proven nor likely to be completely true), an analysis of buoyancy and cloud base temperatures based on soundings can yield a preliminary, very tentative statement on transferability.

For the purpose of this pilot study the analysis will be based on midnight soundings from seven Weather Bureau stations, collected during the 1985/86 PAWS field season for use in daily forecasting for operations (Sect 6, Vol. IV) and the 0600Z Nelspruit sounding. These soundings (for Port Elizabeth, Cape Town, Durban, Upington, Bloemfontein, Alexander Bay and Pretoria) are stored on disk in a database file. It must be emphasized that these are midnight soundings and are from one season only. Also, these "seedability" estimates have a relative value only because they are based on CCL calculations. It is shown in Sect. 6.8 of Vol. IV that the CCL tends to overestimate the buoyancy actually realized (based on the ascent through cloud base, estimated from the Learjet climbout sounding, performed during the convective part of the day). For consistency the morning sounding CCL at Nelspruit has been used in this study.

The following figures (Figs. 6.0-6.3) show plots of cloud base temperature (based on CCL, a forecast) versus the 500 mb buoyancy (Delta T, based on moist adiabatic ascent from the CCL) for the seven stations similar to Fig. 3 of Mather et al., 1986. The solid straight lines in these figures show the bounds of Nelspruit operational days (Delta T at 500 mb greater than $0^{o}C$; cloud base (CCL) temperature greater than $5^{o}C$) and the dividing line between the occurrence of liquid drops at the $-10^{o}C$ level and their non-occurrence. On the same figures appear the total numbers of days in each sample (TD), the number of potential operational days (POD; the number of points in the upper right quadrant), the number of days conducive to the

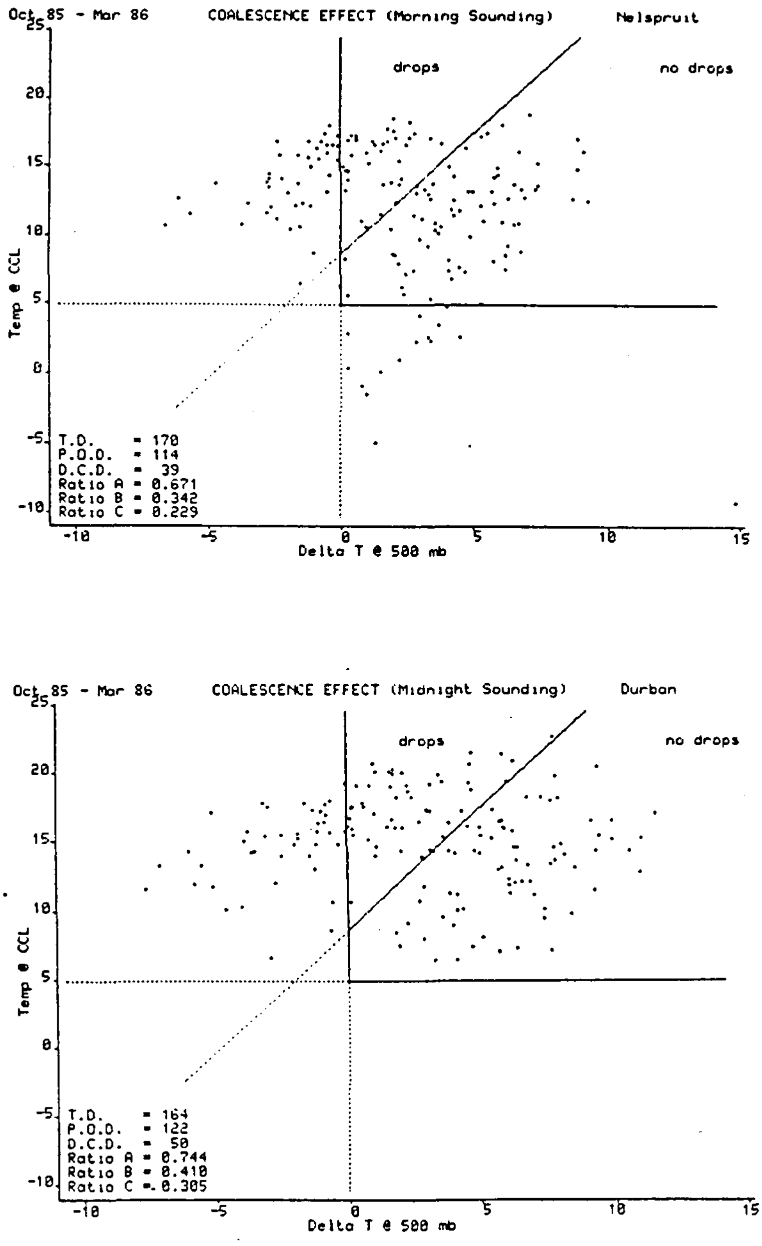

Fig. 6.0. Temperature at CCL versus Delta T at 500 mb for the 1985/86 PAWS operational season, at Nelspruit and Durban.

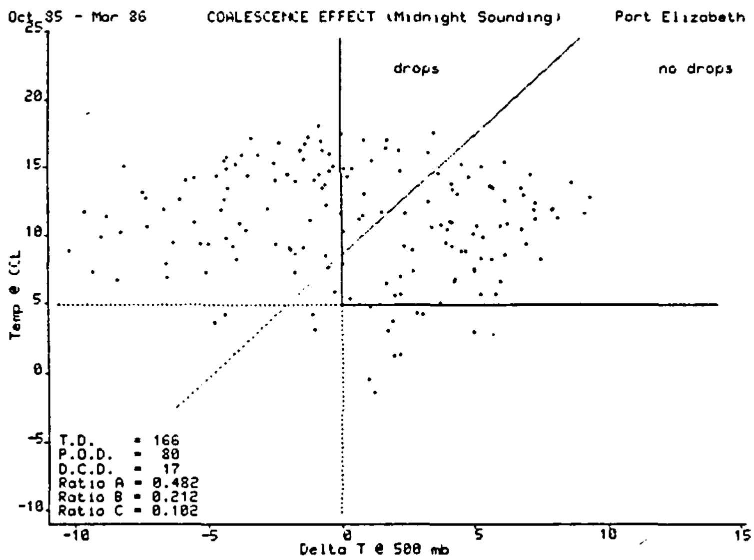

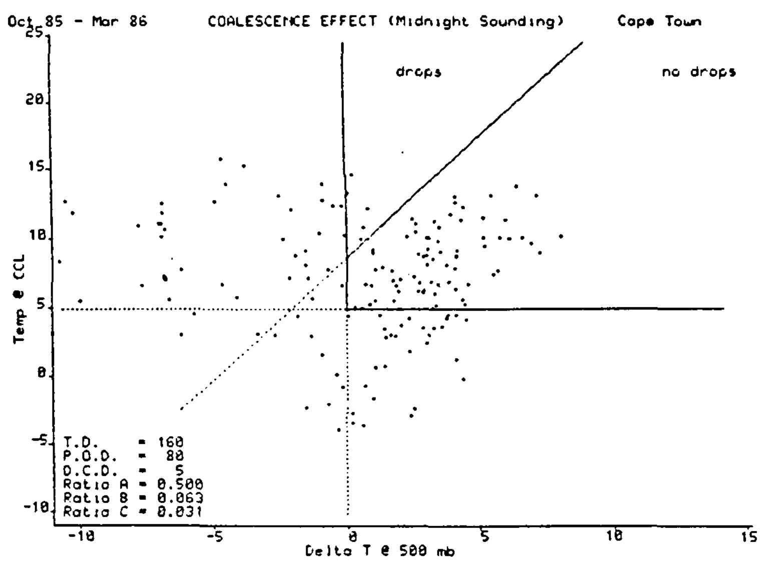

Fig. 6.1. Temperature at CCL versus Delta T at 500 mb for the 1985/86 PAWS operational season, at Port Elizabeth and Cape Town.

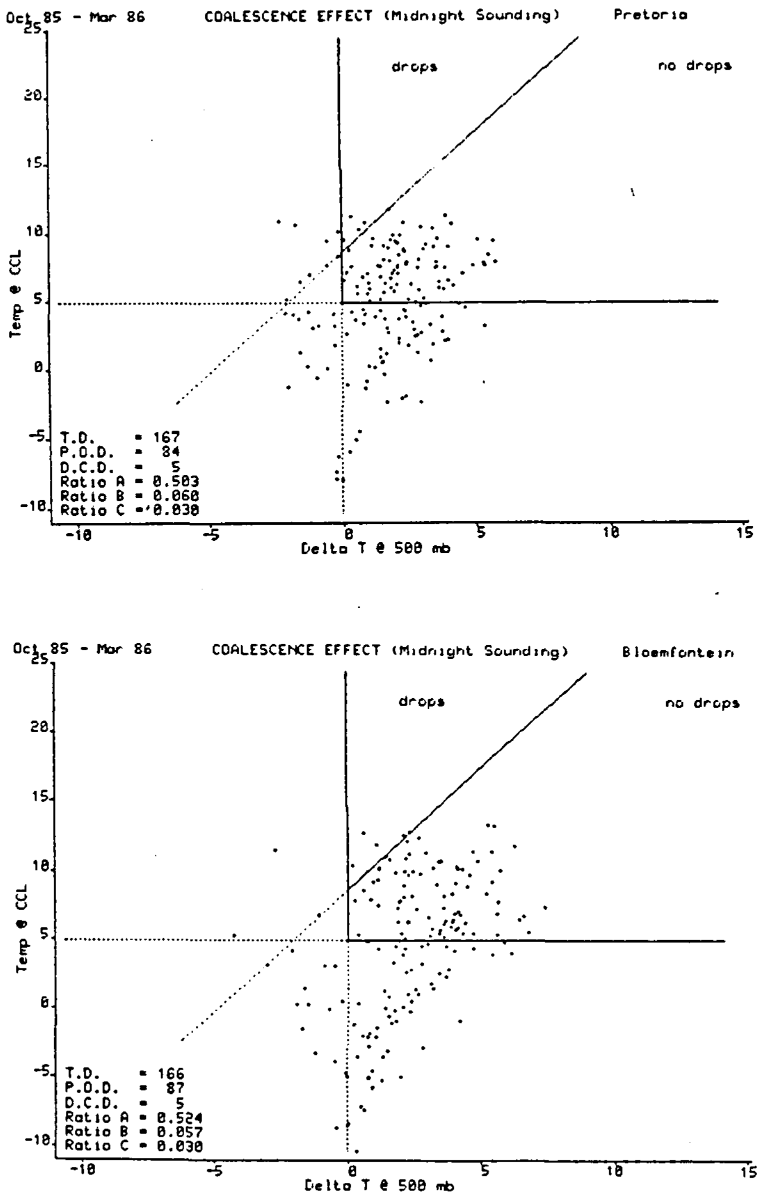

Fig. 6.2. Temperature at CCL versus Delta T at 500 mb for the 1985/86 PAWS operational season, at Pretoria and Bloemfontein.

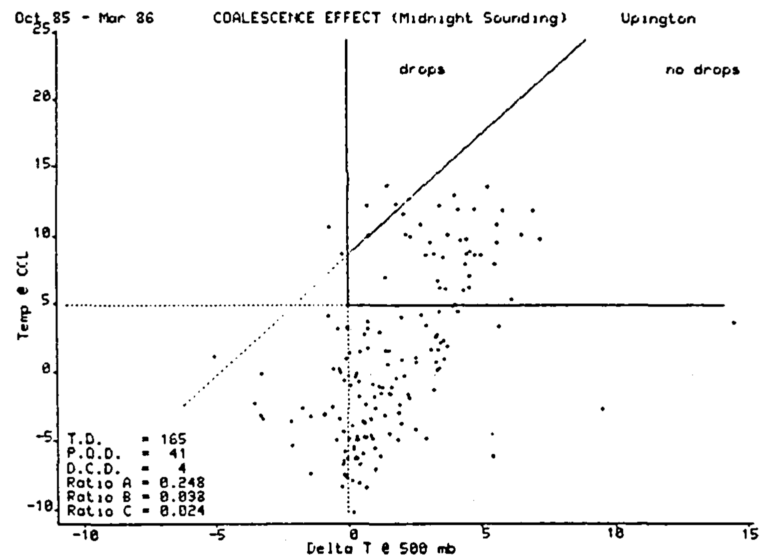

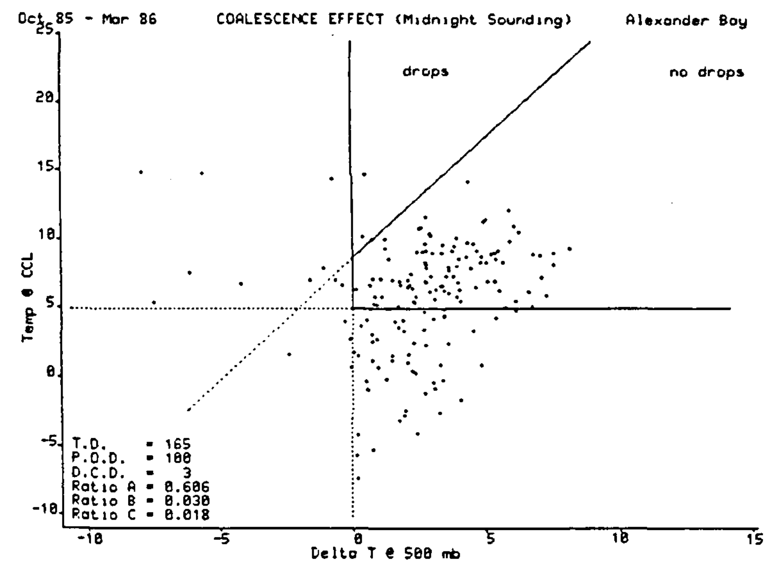

Fig. 6.3. Temperature at CCL versus Delta T at 500 mb for the 1985/86 PAWS operational season, at Upington and Alexander Bay.

occurrence of drops (DCD; that subset of POD above the diagonal dividing line), and the fractions:

Ratio A = POD/TD (probability of operational day)

Ratio B = DCD/POD (probability of drops on an operational day)

Ratio C = DCD/TD (probability of drops on any day).

The values of Ratio B for each of the seven Weather Bureau stations and for Nelspruit have been divided by the value of Ratio B at Nelspruit and these new ratios have been plotted on a national map (Fig. 6.4), permitting a large-scale view of the "relative seedability" or transferability, (based upon the simple assumptions which have been made).

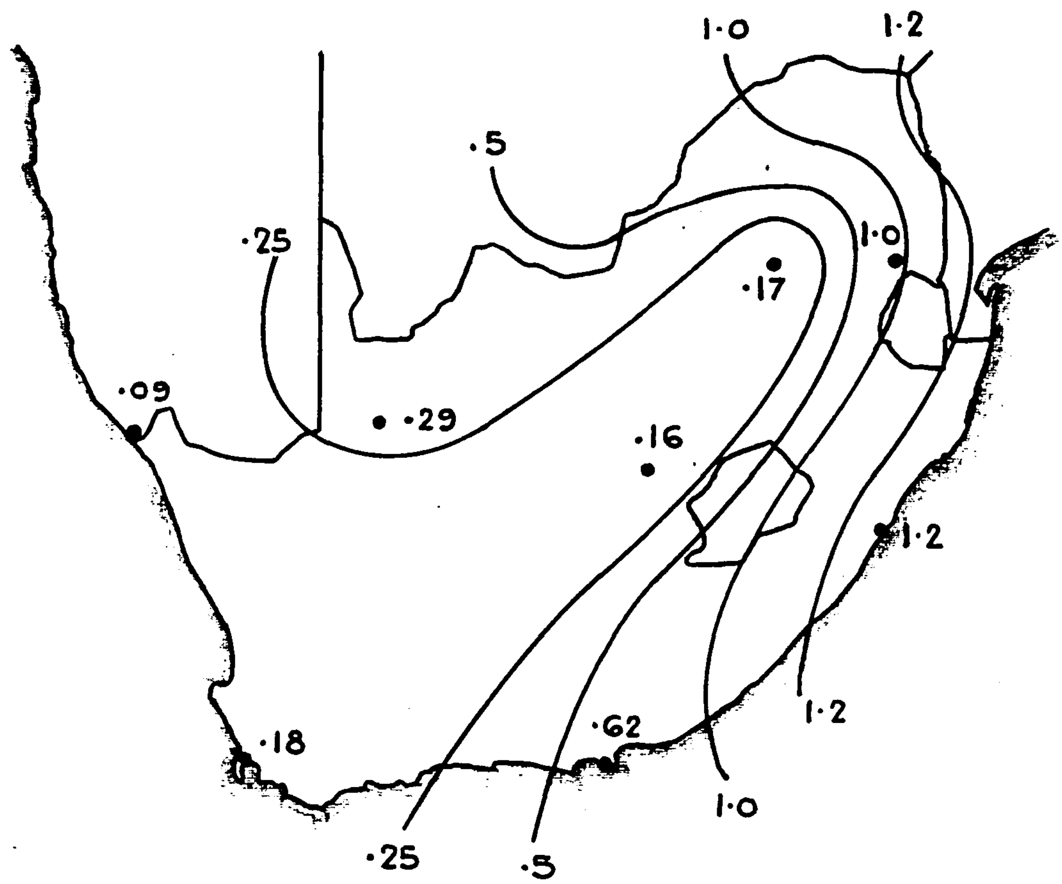

Fig. 6.4. The fraction (Ratio B) of operational days (POD) on which large water drops can be expected at the $-10^{o}C$ level in growing cloud turrets, divided by the value of Ratio B at Nelspruit.

"Seedability" is clearly highest along the east coast and falls off inland. The west coast and the deep interior (Bloemfontein) apparently present few opportunities. The crucial areas for further examination would appear to be intermediate areas.

Note that we have, for the purpose of this study, taken the drop-no drop line as the limit of seedability. This has not been firmly established and further study of this question may lead to a redefinition of seedability. It must be remembered that a cloud can contain a considerable amount of liquid water with no drops appearing on the 2D-C record (see Section 8.0 of Vol IV). Also, the seeding mechanism at Nelspruit is a mixture of dynamic and microphysical effects; purely microphysical effects would have to be evaluated in some other way. An indication of poor seedability in this pilot study does not suggest that rain enhancement is impossible in a given place.

The above is, again, only an illustrative pilot study. The next steps in the determination of transferability would be :

a. extend the study to the noon soundings
b. add the soundings at Pietersburg and Bethlehem to the data sample
c. enlarge the sample to cover five or ten years of soundings
d. determine actual rain and storm days for areas around each sounding site
e. determine natural rainfall amounts for the POD and the DCD for each sounding site.

References

Baumgardner, D., and J.E. Dye, 1982: Cloud particle measurements symposium: Summary and Abstracts. NCAR Tech. Note NCAR/TN - 199, 103pp.

Cooper, W.A., 1978: Cloud physics investigations by the University of Wyoming in Hiplex 1977. Rep. No. AS119, Dept. of Atmos. Sciences, University of Wyoming, 29-31.

Doneaud, A.A., S. Ionescu-Niscov, D.L., Priegnitz and P.L. Smith, 1984: The area time integral as an indicator for convective rain volumes. J. Climate Appl. Meteor., 23, 555-561.

Emmitt, G.D., 1984: Behaviour of cylindrical dry ice pellets - field laboratory and model experiments. Proc. 9th Conf. on Wea. Mod., Park City, 21-23 May, 1984, 20-22.

Gabriel, K.R., and G.K. Mather, 1986: Exploratory data analyses of 1951-82 summer rainfall around Nelspruit, Transvaal, and possible effects of 1972-81 cloud seeding. J. Climate Appl. Meteor., 25, 1077-1087.

Garstang, M., G.D. Emmitt and B. Kelbe, 1981: Rain augmentation in Nelspruit (RAIN). Report to the Water Research Commission, Pretoria, South Africa.

Heymsfield, A.J., and D. Baumgardner, 1985: Summary of a workshop on processing 2-D probe data. Bull. Amer. Meteor. Soc., 66, 437-440.

Hobbs, P.V., and A.L. Rango, 1982: Evidence for the production of ice particles in clouds due to aircraft penetrations. Proc. Conf. on Cloud Physics, Chicago, 1982, 107-110.

Johnson, D.B., 1982: Geographical variations in cloud-base temperature. Preprints Conf. on Cloud Physics. Chicago, Amer. Meteor. Soc., 187-189.

Kahn, A., 1986: Statistical aspects of a weather modification experiment. Unpublished MSc dissertation. University of South Africa, Pretoria.

Knight, N.C., 1981: The climatology of hailstone embryos. J. Appl. Meteor., 20, 750-755.

Lamb, D.J., J. Hallet and R.I. Sax, 1981: Mechanistic limitations to the release of latent heat during the natural and artificial glaciation of deep convective clouds. Quart. J. Roy. Meteor. Soc., 107, 935-954.

Leighton, H.G., and R.R. Rodgers, 1974: Droplet growth by condensation and coalescence in a strong updraft. J. Atmos. Sci., 32, 271-279.

------, and V.A. Pissimanis, 1975: Effects of entrainment and freezing on cloud droplet evolution. Stormy Weather Group Rep. MW-83, McGill University, 00pp

MacCready, P.B., T.B. Smith, C.J. Todd and K.M. Beesmer, 1957: Nuclei, cumulus and seedability studies, Part II. Cumulus studies. Final Rep. of the Advisory Committee on Weather Control, Vol. II, 151-168.

Mather, G.K., B.J. Morrison and G.M. Morgan, Jr., 1986: A preliminary assessment of the importance of coalescence in convective clouds of the Eastern Transvaal. J. Climate Appl. Meteor., 25, 1780-1784.

Morrison, B.J., W.G. Finnegan, R.D. Horn and L.O. Grant, 1984: A laboratory characterization of dry ice as a glaciogenic seeding agent. Proc. 9th Conf. on Wea. Mod. Park City, 21-23 May, 1984, 8-9.

Nelson, L.D., 1979: Observations and numerical simulations of precipitation mechanisms in natural and seeded convective clouds. PhD. dissertation, Dept. of Geographical Sciences, University of Chicago, 188 pp.

Smith, P.L., J.R. Miller, Jr., A.A. Doneaud, J.H. Hirsch, D.L.Priegnitz, P.E. Price, K.J. Tyler and H.D. Orville, 1985: Research to develop evaluation techniques for operational convective cloud modification projects. Report SDSMT/IAS/R-85/02. Institute of Atmospheric Science, S. Dakota School of Mines and Technology, 93 pp.

Tsonis, A.A., G.L. Austin and S. Lovejoy, 1984: A proposal for a new statistic and technique development for the design and evaluation of cloud seeding experiments. Atmpsphere Ocean 22, 67-82.

Young, K.C., 1974: The evolution of drop spectra through condensation, coalescence and breakup. Proc. Conf. on Cloud Physics, Tucson, Amer. Meteor. Soc., 95-98.